Structure−Activity Relationships of a Novel Class of Endothelin-A Receptor Antagonists and Discovery of Potent and Selective Receptor Antagonist, 2-(Benzo[1,3]dioxol-5-yl)-6-isopropyloxy-4-(4-methoxyphenyl)-2*H*-chromene-3-carboxylic Acid (S-1255). 1. Study on Structure−Activity Relationships and Basic Structure Crucial for ET_A Antagonism

Natsuki Ishizuka,* Ken-ichi Matsumura, Katsunori Sakai, Masafumi Fujimoto, Shin-ichi Mihara, and Teruo Yamamori

Shionogi Research Laboratories, Shionogi & Co., Ltd., 12-4, Sagisu 5-chome, Fukushima-ku, Osaka 553-0002, Japan

Received August 10, 2001

A novel series of endothelin-A (ET_A) selective receptor antagonists having a 2*H*-chromene skeleton are described. A lead compound, 2-(benzo[1,3]dioxol-5-yl)-2*H*-chromene-3-carboxylic acid (**3**), was found by modifications of our own angiotensin II antagonist. A structure−activity relationship (SAR) study of **3** reveals that the structural requirements essential for potent and selective ET_A receptor binding affinity are the *m*,*p*-methylenedioxyphenyl, carboxyl, and isopropoxy groups at the 2-, 3-, and 6-positions, respectively, on the (*R*)-2*H*-chromene skeleton. The substituent at the 4-position is also important for improving the activity, and various hydrophobic functional groups of 6−9 Å such as liner, branched, and cyclic aliphatic groups, unsubstituted and substituted aryl groups, and even halogen atoms were acceptable. These results suggest that (*R*)-2-(benzo[1,3]dioxol-5-yl)-6-isopropoxy-2*H*-chromene-3-carboxylic acid, formula **108**, is the crucial basic structure to be recognized by the ET_A receptor. The most potent compound is (*R*)-**48** (S-1255), which binds to the ET_A receptor with an IC_{50} value of 0.19 nM and is 630-fold selective for the ET_A receptor than for the ET_B receptor. This compound has 55% oral bioavailability in rats. On the basis of the SAR, the roles of each substituent in the receptor binding are discussed.

Introduction

The endothelins (ETs) were isolated from porcine aortic endothelial cells by Yanagisawa and co-workers in 1988.[1] To date, three isopeptides, ET-1, ET-2, and ET-3, have been identified.[2] They are 21 amino acid peptides with two disulfide linkages (1−15 and 3−11) and conserve high homology sequences to each other, especially where hydrophobic C-terminals are completely conserved. The mature ETs are synthesized from big endothelins, of which Trp_{21}−Val_{22} are cleaved by the endothelin converting enzyme (ECE).[3,4] ET-1 is the most potent vasoconstrictor peptide known and has a long duration of action.

ET receptors belong to a seven transmembrane G-protein-coupled receptor (7TM/GCPR) family,[5,6] and two receptor subtypes, endothelin A (ET_A) and endothelin B (ET_B), have been identified.[7,8] The ET_A receptor binds to three isopeptides with affinities in the order of ET-1 = ET-2 > ET-3, while the ET_B receptor binds equally to them.[6] The ET_A receptor is mainly expressed on vascular smooth muscle cells[5] and causes vasoconstriction. On the other hand, the ET_B receptor on endothelial cells causes vasodilatation through the production of endothelium-derived relaxing factors (EDRF): nitric oxide (NO) and prostacyclins. The ET_B receptor also is expressed on vascular smooth muscle cells and causes vasoconstriction as the ET_A receptor does.[9] However, the roles of the ET_B receptor have not been fully characterized. Recently, an ET-3 specific receptor, ET_C, was identified from *Xenopus laevis* dermal melanophores,[10] but the existence of ET_C in mammalian tissue is unknown.

In mammals, ET receptors are distributed in a wide variety of tissues, and elevated levels of the plasma concentration of ET-1 were observed in several diseases such as hypertension,[11,12] pulmonary hypertension,[13,14] acute myocardial infarction,[15] congestive heart failure,[16,17] renal failure,[18,19] and atherosclerosis.[20] This observation suggests the relevance of ETs to pathogenesis of such diseases. In fact, blocking of ETs using a monoclonal antibody or ET receptor antagonists in animal pathological models showed an antihypertensive activity in hypertension,[21,22] reduction of the myocardial infarct size in acute myocardial ischemia and reperfusion,[23,24] reduction in neointimal formation in a carotid artery balloon angioplasty model,[25] improvement of survival in chronic heart failure,[26] and improvement of the glomerular filtration rate in acute ischemic renal failure.[27] In human clinical trials of chronic heart failure patients, intravenous administration of a nonpeptidic antagonist Ro 47-0203 (Bosentan)[28,29] reduced their blood pressure and improved their cardiac performance.[30] These results strongly indicate that blocking the ET receptors is a powerful therapeutic strategy in ameliorating various disease states and ET antagonists could be promising new therapeutic agents.

* To whom correspondence should be addressed. Tel.: +81(6)6458-5861. Fax: +81(6)6458-0987. E-mail:natsuki.ishizuka@shionogi.co.jp.

10.1021/jm010382z CCC: $22.00 © 2002 American Chemical Society
Published on Web 04/09/2002

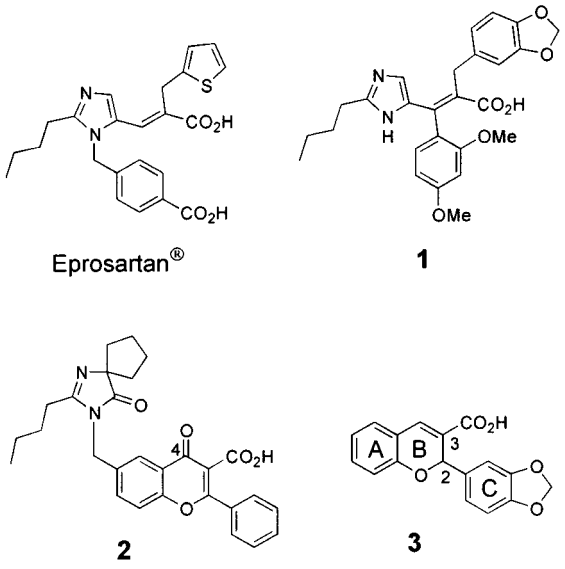

Figure 1.

Early developments of ET antagonists were initiated using peptidic compounds. They include BQ-123,[31,32] FR139317,[33] BQ-788,[34] RES-701-1,[35] IRL-1038,[36] PD142893,[37] PD145065,[38] and TAK-044.[39] On the other hand, the first nonpeptidic antagonist, Ro 46-2005,[40] was disclosed in 1993 by the Roche group. Now, many highly potent nonpeptidic antagonists such as BMS-182874,[41,42] SB-209670,[43,44] PD-156707,[45,46] A-127722,[47,48] Bosentan,[28,29] L-754142,[49,50] and A-182086[51] are known. Some are selective antagonists for ET_A receptors, and others act on both ET_A and ET_B receptors. Although it remains unclear at present which type of antagonists, selective ET_A or mixed ET_A/ET_B, is more suitable for the clinical purposes,[52,53] these facts prompted us to develop novel nonpeptide ET receptor antagonists.

A literature survey at the start of the ET project revealed that various chemical structures, derived from both synthetic and natural resources, were reported to act on ET receptors. Among them, we were very interested in a series of compounds disclosed in a patent by the SmithKline-Beecham group.[54] These compounds, for example, **1**, were apparently synthesized during the course of development of angiotensin II (AII) receptor antagonists because their structures are closely related to their AII receptor antagonist, Eprosartan[55,56] (Figure 1). This prompted us to modify our own AII receptor antagonists, and compound **2** was one of such starting materials. Fortunately, we found very weak affinity for the ET_A receptor in compound **3**, which was obtained by the modification of the partial structure of **2**.

In this paper, we will describe the discovery of our lead compound **3** and the structure−activity relationships (SAR) of its derivatives leading to our clinical candidate (*R*)-**48**. Also discussed are the essential roles of substituents at the 2-, 3-, 4-, and 6-positions of the 2*H*-chromene skeleton.

Chemistry

The 4-alkoxy, 4-aryl, and 4-unsubstituted derivatives, listed in Tables 1−4 (**11**−**33**, **36**−**79**, **3**, and **82**), were synthesized via key intermediate **9** as outlined in Scheme 1. The Vilsmeier−Haack reaction of alkoxy-2-hydroxyacetophenones **5**, which were commercially avairable or synthesized from dihydroxyacetophenone **4** and an alkyl halide, gave 3-formyl derivatives **6**.[57] Oxidation of the formyl group of **6** with sodium chlorite[58] and successive esterification gave esters **8**. The Michael addition of an appropriate Grignard reagent to **8** in the presence of copper(I) iodide proceeded exclusively at the 2-position to give the key intermediates **9** as a mixture of keto−enol tautomers, **9a**,**b**.

Introduction of an alkoxy group at the 4-position was carried out by the Mitsunobu reaction of intermediates **9** with an appropriate alcohol. Alkaline hydrolysis of the resulting esters **10** gave 4-alkoxy acids **11**−**33**.

Introduction of an aryl group at the 4-position was accomplished by reaction of **9** with 2-[*N*,*N*′-bis(trifluoromethanesulfonyl)amino]pyridine, followed by the Suzuki coupling reaction of the resulting triflate **34** and an appropriate boronic acid. Subsequent alkaline hydrolysis provided 4-aryl acids **36**−**79**.

Hydrogenation of intermediates **9** over 10% Pd/C in ethyl acetate yielded 4-hydroxy esters **80**. Dehydration of **80** with a catalytic amount of *p*-toluenesulfonic acid in refluxing toluene afforded 4-unsubstituted esters **81**, which were converted into 4-unsubstituted acids **3** and **82** by alkaline hydrolysis.

The 4-alkyl derivatives, **83**−**92**, shown in Table 4 were synthesized from 4-methoxy acid **22** (Scheme 2). Thus, addition of an alkyl Grignard reagent to **22** at low temperature gave the corresponding 4-alkyl acids **83**−**92**.

Scheme 3 shows the synthetic routes for 4-chloro, 4-butylthio, and 4-phenoxy derivatives **95**, **96**, and **98**, respectively. Regioselective alkylation of 2,5-dihydroxyacetophenone **4a** with 2-bromopropane and successive condensations of the resulting acetophenone **5a** with piperonal under aqueous basic conditions provided chromanone **93**. Treatment of **93** with phosphorus oxychloride in dimethylformamide (DMF) caused formylation at the 3-position and chlorination at the 4-position simultaneously, giving 4-chloro-3-formyl intermediate **94** in good yield.[59] Oxidation of the formyl group of **94** with sodium chlorite gave 4-chloro acid **95**, which was further converted into 4-*n*-butylthio acid **96** by reaction with sodium butanethiolate.

Addition of sodium *p*-methoxyphenoxide to 4-chloro-3-formyl intermediate **94** yielded 4-phenoxy-3-formyl compound **97**. Oxidation of the formyl group of **97** with sodium chlorite under buffered conditions (pH = 5) smoothly proceeded to give 4-phenoxy acid **98** in good yield.

Modifications of the carboxylic acid at the 3-position in 4-*n*-butyl acid **83** and 4-*p*-anisyl acid **48** are shown in Scheme 4. Reaction of acid **83** with oxalyl chloride, followed by treatment with methanol, yielded the corresponding 4-*n*-butyl ester **99**. Successive treatment of acids **83** and **48** with oxalyl chloride and with 28% NH_4-OH afforded corresponding amide derivatives **100** and **101**, respectively. Amide **100** was further converted into tetrazole **102** by reaction with sodium azide and tetrachlorosilane.[60] 3-Acylsulfonamide derivatives **103** and **104** were synthesized by condensation of acids **83** and **48** with methanesulfonamide using the carbodiimide-4-(dimethylamino)pyridine method.[61]

Scheme 5 shows the synthesis of 3,4-dihydro compounds **106** and **107** listed in Table 6. Catalytic hydro-

Scheme 1[a]

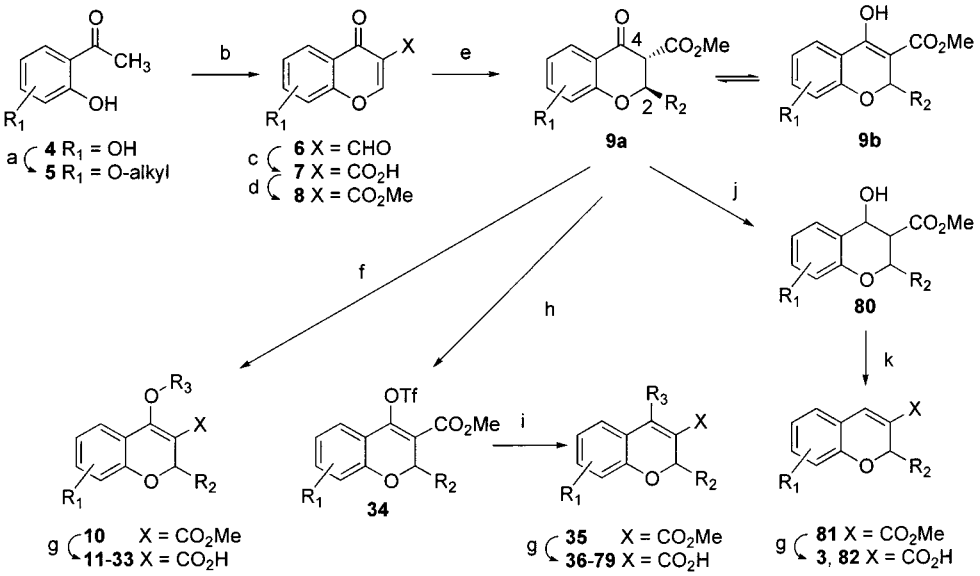

[a] Reagents: (a) Alkyl halide, K_2CO_3, KI, DMF. (b) $POCl_3$, DMF. (c) $NaClO_2$, H_2NSO_3H, CH_2Cl_2, H_2O. (d) (i) $(COCl)_2$, CH_2Cl_2; (ii) CH_3OH. (e) R_2MgBr or R_2MgCl, CuI, THF. (f) R_3OH, diethyl azodicarboxylate, PPh_3, THF. (g) 1 M NaOH, THF, CH_3OH. (h) 2-[*N*,*N*′-bis(trifluoromathanesulfonyl)amino]pyridine, NaH, DMF. (i) $R_3B(OH)_2$, $Pd(PPh_3)_4$, 2 M Na_2CO_3, DME. (j) H_2, 10% Pd/C, EtOAc. (k) *p*-TsOH, toluene.

Scheme 2[a]

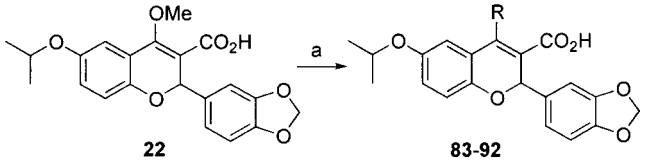

[a] Reagents: (a) RMgBr or RMgCl, THF.

genation of esters **99** and **35a** afforded corresponding dihydro esters **105**, whose all cis configurations were determined by ^{1}H nuclear magnetic resonance (NMR) coupling constants: $J_{2,3} = 2-3$ Hz and $J_{3,4} = 6-7$ Hz, respectively. Alkaline hydrolysis of **105** proceeded with epimerization at the 3-position to give all trans acids **106** and **107** exclusively. Their stereochemistry was established on the basis of ^{1}H NMR coupling constants: $J_{2,3} = 9-11$ Hz and $J_{3,4} = 10-12$ Hz.

4-*p*-Anisyl acid **48** was resolved into its enantiomers (+)-**48** and (−)-**48** via (1*S*,2*R*)-(+)- and (1*R*,2*S*)-(−)-norephedrine salts, respectively. Absolute configurations of (+)-**48** and (−)-**48** were assigned to be *R* and *S*, respectively, on the basis of the single-crystal X-ray structure of the (1*S*,2*R*)-(+)-norephedrine salt of (+)-**48** (Figure 2). 4-Unsubstituted acid **82** was resolved into the enantiomers (−)-**82** and (+)-**82** via (*S*)-(−)- and (*R*)-(+)-phenylethylamine salts, respectively, whose absolute configurations were determined by comparison of their CD spectra with the CD spectrum of (*R*)-**48**. (*R*)-**48** and (−)-**82** exhibited positive Cotton effects around 240 nm owing to the $\pi-\pi^*$ transition of the styrene chromophore. This observation indicates that the stereochemistry of both compounds is the same and thus the absolute configuration of (−)-**82** is *R*.[62]

Optical resolution of 4-methoxy acid **22** with (1*S*,2*R*)-(+)-norephedrine gave (+)-**22**. Because (+)-**22** was converted into (*R*)-**48** by reaction with *p*-anisylmagnesium bromide (Scheme 6), the *R*-configuration of (+)-**22** was established also. (*R*)-4-*n*-Butyl acid, (*R*)-**83**, was synthesized from (*R*)-**22** and *n*-butyl magnesium chloride as shown in Scheme 6.

Optical purities of all of the chiral compounds listed in Table 7 were confirmed to be more than 98% ee by chiral high-performance liquid chromatography (HPLC) analysis. In the following discussion, the three rings are named as the A-, B-, and C-rings as shown in Figure 1.

Biological Testing

The binding affinities for the rat ET_A and pig ET_B receptors of the synthesized compounds were determined by their inhibition of the [^{125}I]ET-1 binding in rat aorta smooth muscle cells and the [^{125}I]ET-3 binding to the cloned pig ET_B receptor expressed in COS-7 cells, respectively.[63] The binding studies for human receptors were performed in a similar fashion, using human ET_A and ET_B receptors expressed in Chinese hamster ovary (CHO) cells.[63] The upper limits of the IC_{50} values determined for the ET_A or ET_B receptor bindings were 100 μM. The results are summarized in Tables 1−7.

Results and Discussion

(1) Finding of Lead Compound. As described in the Introduction, our initial efforts to find a lead compound of a novel series of ET receptor antagonists were focused on various AII antagonists, including **2** and related analogues. Fortunately, 2*H*-chromene **3** obtained by reduction of the 4-carbonyl group of the flavone substructure of **2** showed very weak binding affinity to the ET_A receptor ($IC_{50} = 67$ μM, Figure 1). The simple tricyclic structure of **3** offered plenty of room for chemical modifications to increase activity, and thus, **3** was selected as our first lead compound.

Surprisingly, introduction of an alkoxy group at the 4-position in **3**, which was readily made by treatment of **9** with an alcohol under Mitsunobu conditions, dramatically increased the binding affinity for the ET_A receptor (Table 1). As the chain length of the 4-alkoxy group was increased, the affinity was improved. The

Scheme 3[a]

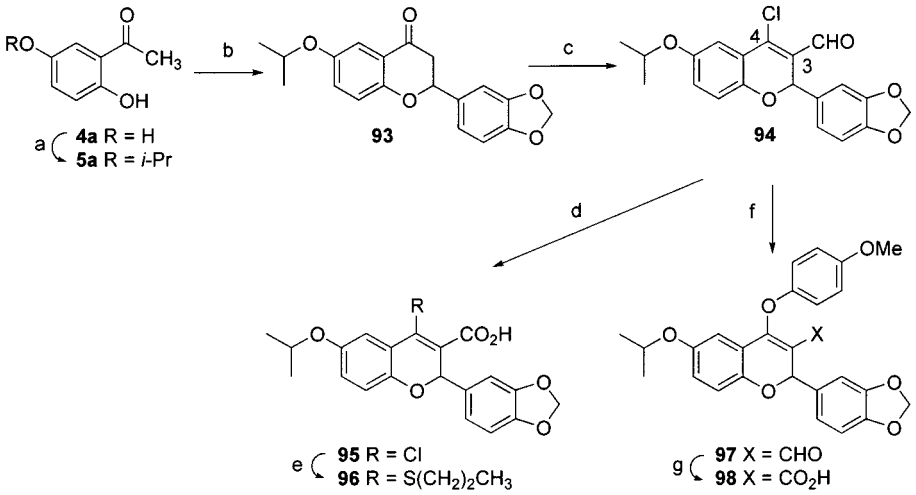

[a] Reagents: (a) 2-Bromopropane, K_2CO_3, CH_3CN. (b) Piperonal, 2 M NaOH, MeOH. (c) $POCl_3$, DMF. (d) $NaClO_2$, H_2NSO_3H, toluene, H_2O. (e) 1-Butanethiol, NaH, THF. (f) 4-Methoxyphenol, NaH, DMF. (g) $NaClO_2$, NaH_2PO_4, CH_3CN, H_2O.

Scheme 4[a]

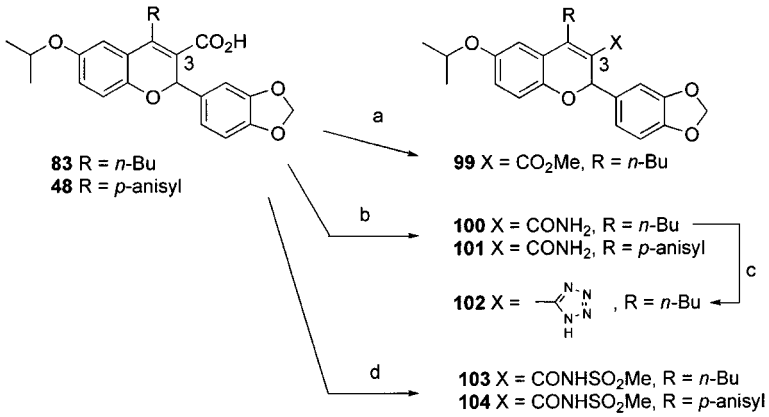

[a] Reagents: (a) (i) $(COCl)_2$, catalytic DMF, CH_2Cl_2; (ii) CH_3OH. (b) (i) $(COCl)_2$, catalytic DMF, CH_2Cl_2; (ii) 28% NH_4OH. (c) NaN_3, $SiCl_4$, CH_3CN. (d) Methanesulfonamide, *N*-ethyl-3-(3-dimethylaminopropyl)carbodiimide hydrochloride, 4-(dimethylamino)pyridine, CH_2Cl_2.

Scheme 5[a]

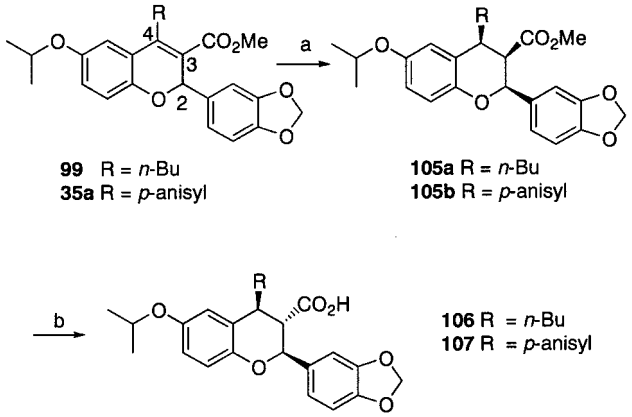

[a] Reagents: (a) H_2 (500 kPa), 5% Pd/C, AcOH, THF, EtOAc or H_2 (500 kPa), $PdCl_2$, MeOH, $CHCl_3$. (b) 1 M NaOH, THF, MeOH or 1 M NaOH, DMSO.

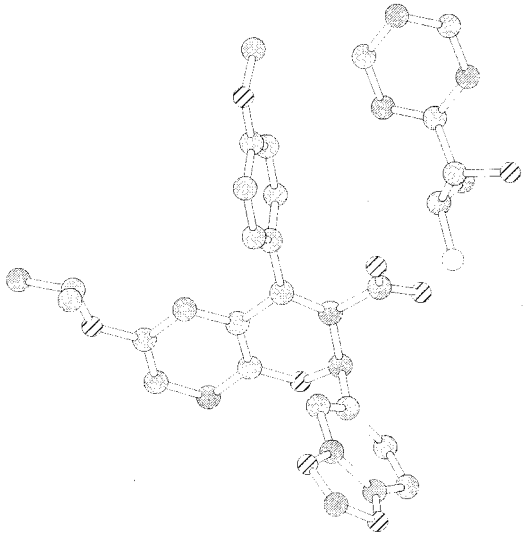

Figure 2. Single-crystal X-ray structure of (*R*)-**48** as (1*S*,2*R*)-(+)-norephedrine salt. All hydrogens are removed for clarity.

n-butoxy and *n*-pentoxy derivatives **13** and **14** were approximately 1000 times more potent than the lead compound **3**.

Introduction of the phenyl or substituted phenyl group at the 4-position, which was routinely achieved by the Suzuki coupling reaction of triflate **34** and an appropriate boronic acid, also resulted in dramatic increases in the binding affinity for the ET_A receptor. *p*-Anisyl and *p*-isopropylphenyl groups (**39** and **42**) were found to be the most effective substituents, giving the affinities

Scheme 6[a]

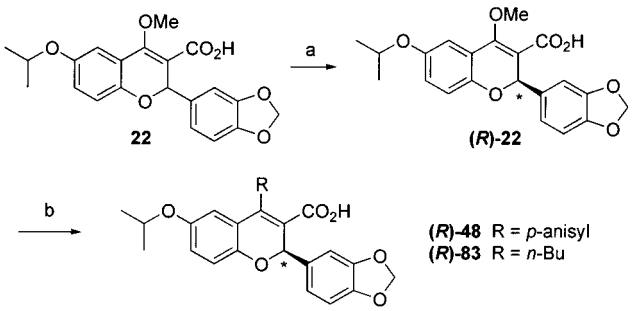

[a] Reagents: (a) (1*S*,2*R*)-(+)-Norephedrine, CH_3OH. (b) RMgBr or RMgCl, THF.

Table 1. Substituent Effect at the 4-Position

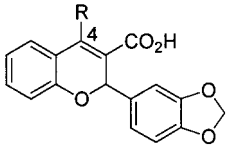

		IC_{50} (nM)[a]	
compd	R	$r ET_A$[b]	$p ET_B$[c]
3	H	67000 ± 4000 (2)	>100 000 (1)
11	OC_2H_5	290 ± 20 (2)	15 000 ± 5000 (2)
12	O-*n*-C_3H_7	160 ± 20 (2)	10 000 (1)
13	O-*n*-C_4H_9	66 ± 0 (2)	4900 (1)
14	O-*n*-C_5H_{11}	29 ± 7 (2)	1100 ± 290 (2)
36	C_6H_5	780 ± 20 (2)	>100 000 (1)
37	2′-$CH_3OC_6H_4$	2200 ± 900 (2)	31 000 (1)
38	3′-$CH_3OC_6H_4$	700 (1)	2800 (1)
39	4′-$CH_3OC_6H_4$	86 ± 14 (2)	1400 (1)
40	3′,4′-(−OCH_2O−)C_6H_3	350 (1)	710 ± 160 (2)
41	4′-$CH_3C_6H_4$	530 ± 50 (2)	6900 ± 1100 (2)
42	4′-*i*-$C_3H_7C_6H_4$	83 ± 3 (2)	2100 ± 400 (2)
43	4′-ClC_6H_4	800 ± 100 (2)	5800 ± 200 (2)

[a] A mean IC_{50} value ± standard error of the mean (SEM) with the number of experiments given in parentheses. [b] Rat receptors. [c] Pig receptors.

similar to those of *n*-butoxy and *n*-pentoxy groups (**13** and **14**). The other substituted phenyl derivatives were less potent than **39** and **42**, though considerably more potent than the lead compound **3**.

Because these two types of 4-substituted compounds, the 4-alkoxy and 4-aryl series, seemed to be equally promising, compounds **13** and **39** having structurally distinct 4-substituents were selected as the second lead compounds for further chemical modifications.

In contrast to the satisfactory improvement in the binding affinity for the ET_A receptor, that for the ET_B receptor was not significant. In the following section, we will thus focus our discussion on the ET_A receptor binding affinity.

(2) Substituent Effect on A-Ring. Substituent effects on the A-ring for the ET receptor binding affinity were examined in the second lead compounds **13** and **39** (Table 2). In both series of compounds, introduction of an alkoxy group at the 6-position gave an equal to significantly improved affinity (**16**−**20** or **45**−**51**). In each of these cases, close correlation was observed between the chain length and the affinity for the ET_A receptor. The optimal number of the carbon atoms is 2−4 (**17**−**20** or **46**−**49**), and with a shorter or longer group such as methoxy (**16** and **45**) or benzyloxy (**50**), the binding affinity diminishes greatly. Among these groups, the branched isopropoxy group was especially effective, giving highly potent derivatives **19** and **48** with the IC_{50} values of less than 1 nM, which were 100 times more potent than the second lead compounds **13** and **39**, respectively. Insertion of a terminal hydroxyl group into the isopropoxy group led to a slight loss in the activity (**51**). Importantly, removal of the oxygen atom from the isopropoxy group drastically diminished the activity (**52**), suggesting that this oxygen atom is important not only as a spacer but also as a pharmacophore that acts as a hydrogen-bonding acceptor at the receptor active site. In contrast to the 6-position SAR, introduction of a similar alkoxy group at the 5-, 7-, or 8-position resulted in a significant loss in the activity (**15**, **21**, **44**, **53**, and **54**). These results indicate that the alkoxy group at the 6-position, especially the isopropoxy group, is essential for the potent binding affinity. It is suggested that the 6-isopropoxy group is properly recognized by the ET_A receptor with its isopropyl part acting as a hydrophobic region and its oxygen atom acting as a hydrogen-bonding acceptor.

Introduction of an alkoxy group at the 6-position also improved the binding affinity for the ET_B receptor, but the effect was limited (IC_{50} > 130 nM). As a result, the selectivity for the ET_A receptor became large. The most significant compounds, **19** and **48**, are 1900 and 350 times selective for the ET_A receptor over the ET_B receptor, respectively, and thus, they selectively bound to the ET_A receptor.

(3) Substituent Effect at 2-Position. Substituent effects on the 2-phenyl ring were examined by using compounds shown in Table 3, which had different substituent patterns at the 4- and 6-positions. As shown in the table, replacement of the *m*,*p*-methylenedioxy group by another functional group such as an *o*-, *m*-, or *p*-alkoxy, alkyl, or hydroxyl group consistently diminished the affinity for the ET_A receptor, indicating that the *m*,*p*-methylenedioxy group is exclusively effective on the 2-phenyl ring.

Interestingly, some *o*,*p*-dimethoxy (**57** and **65**) and *p*-methoxy compounds (**58** and **69**) retained moderate affinities. As compared with these compounds, the affinities of the corresponding *o*,*m*-dimethoxy (**66**), *o*- or *m*-methoxy (**67** or **68**), and *p*-alkyl (**59**) derivatives were very weak. This observation suggests that the oxygen atom at the *p*-position on the 2-phenyl ring plays a crucial role as a hydrogen-bonding acceptor at the receptor binding site. Cleavage of the methylenedioxy bridge (**55**, **56**, and **64**) and introduction of a bulkier alkoxy group at the *p*-position (**70** and **71**) also drastically diminished the affinity, suggesting that the sterically less-hindered and conformationally restricted methylendioxy group is advantageous for forming a hydrogen bond with the ET_A receptor active site.

Interestingly, a combination of the *m*,*p*-methylenedioxyphenyl group and the *n*-propyl or *n*-butyl group at the 4- and 6-positions, respectively, tended to improve the affinity for the ET_B receptor (**62**, **63**, **65**, and **69**), although their binding affinities were still unsatisfactory. This tendency suggests a possibility that ET_A/ET_B-balanced antagonists could be found by modifications of these compounds. In this paper, however, no further discussion will be made on this subject.

Table 2. Substituent Effect on the A-Ring

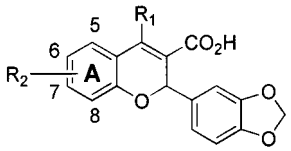

compd	R_1	R_2	IC_{50} (nM)[a] rET_A[b]	IC_{50} (nM)[a] pET_B[c]	B/A[d]
13	O-*n*-C_4H_9	H	66 ± 0 (2)	4900 (1)	74
15		5-O-*n*-C_3H_7	3400 (1)	6000 ± 300 (2)	1.8
16		6-OCH_3	250 (1)	2300 ± 200 (2)	9.2
17		6-OC_2H_5	4.2 ± 0.2 (2)	1600 ± 200 (2)	380
18		6-O-*n*-C_3H_7	2.0 (1)	520 ± 70 (2)	260
19		6-O-*i*-C_3H_7	0.41 ± 0.01 (2)	780 (1)	1900
20		6-O-*n*-C_4H_9	3.0 ± 1.0 (2)	470 ± 90 (2)	160
21		7-O-*n*-C_3H_7	180 ± 40 (2)	2800 ± 200 (2)	16
39	4′-$CH_3OC_6H_4$	H	86 ± 14 (2)	1400 (1)	16
44		5-O-*n*-C_3H_7	1200 ± 480 (2)	1800 ± 200 (2)	1.5
45		6-OCH_3	74 ± 11 (2)	540 ± 20 (2)	7.3
46		6-OC_2H_5	3.8 ± 0.5 (2)	400 ± 20 (2)	110
47		6-O-*n*-C_3H_7	4.4 (1)	220 ± 20 (2)	50
48		6-O-*i*-C_3H_7	0.51 ± 0.04 (2)	180 (1)	350
49		6-O-*n*-C_4H_9	17 ± 1 (2)	130 ± 10 (2)	7.6
50		6-$OCH_2C_6H_5$	62 ± 14 (2)	790 (1)	13
51		6-$OCH(CH_3)CH_2OH$	2.8 ± 0.8 (2)	170 ± 10 (2)	61
52		6-*i*-C_3H_7	110 ± 40 (2)	190 (1)	1.7
53		7-O-*n*-C_3H_7	970 ± 40 (2)	2300 ± 300 (2)	2.4
54		8-OCH_3	1600 (1)	4000 ± 500 (1)	2.5

[a−c] See footnotes a−c of Table 1. [d] $IC_{50}(ET_B)/IC_{50}(ET_A)$.

Table 3. Substituent Effect at the 2-Position

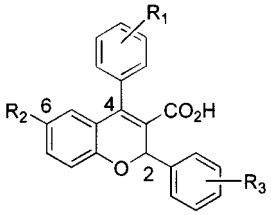

compd	R_1	R_2	R_3	IC_{50} (nM)[a] rET_A[b]	IC_{50} (nM)[a] pET_B[c]
48	4′-OCH_3	O-*i*-C_3H_7	3′,4′-OCH_2O-	0.51 ± 0.04 (2)	180 (1)
55			3′,4′-$(OH)_2$	440 ± 20 (2)	>100 000 (2)
56			3′,4′-$(OCH_3)_2$	170 ± 70 (2)	NT[d]
57			2′,4′-$(OCH_3)_2$	8.0 ± 2.0 (2)	770 ± 10 (2)
58			4′-OCH_3	35 ± 5 (2)	1300 (1)
59			4′-*i*-C_3H_7	1200 ± 200 (2)	5900 (1)
60	3′,4′-OCH_2O-	O-*i*-C_3H_7	3′,4′-OCH_2O-	3.2 ± 0.2 (2)	170 ± 80 (2)
61			4′-*i*-C_3H_7	1300 (1)	2700 (1)
62		O-*n*-C_3H_7	3′,4′-OCH_2O-	43 (1)	80 (1)
63			4′-CH_3O	220 ± 0 (2)	72 ± 5 (2)
64		O-*n*-C_4H_9	3′,4′-$(OCH_3)_2$	810 ± 140 (2)	400 ± 50 (2)
65			2′,4′-$(OCH_3)_2$	18 (1)	35 ± 8 (2)
66			2′,5′-$(OCH_3)_2$	160 ± 40 (2)	1600 (1)
67			2′-OCH_3	130 (1)	760 ± 170 (2)
68			3′-OCH_3	350 (1)	160 ± 40 (2)
69			4′-OCH_3	95 (1)	43 ± 7 (2)
70			4′-O-*n*-C_4H_9	5200 ± 600 (2)	3600 (1)
71			4′-O-*c*-C_5H_9	4800 ± 600 (2)	2200 (1)

[a−c] See footnotes a−c of Table 1. [d] NT = not tested

(4) Substituent Effect at 4-Position. Preliminary SAR studies on the substituent effect at the 4-position (Table 1) indicate that introduction of the structurally distinct aliphatic and aryl groups were equally effective for increasing the affinity. To understand why these distinct groups are acceptable at the 4-position, the substituent effects at this position were reinvestigated in detail, fixing the 2- and 6-substituents to the most promising groups, the *m*,*p*-methylenedioxyphenyl and isopropoxy groups, respectively.

Table 1 reveals that the affinity tends to increase with increasing chain length of the 4-alkoxy group. To investigate the optimal length of the 4-substituent, linear alkoxy groups from methoxy (**22**) to decyloxy (**28**) were systematically introduced into the parent 4-unsubstituted compound **82**. The results in Table 4 show

Table 4. Substituent Effect at the 4-Position

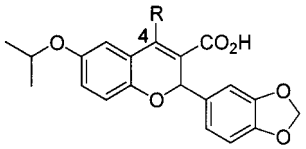

compd	R	IC50 (nM)[a] rET_A[b]	IC50 (nM)[a] pET_B[c]
82	H	330 ± 30 (2)	52 000 ± 14 000 (2)
22	OCH_3	9.1 ± 0.1 (2)	6400 (1)
23	OC_2H_5	2.2 (1)	2800 (1)
24	O-*n*-C_3H_7	1.5 ± 0.2 (2)	1300 (1)
19	O-*n*-C_4H_9	0.41 ± 0.01 (2)	780 (1)
25	O-*n*-C_5H_{11}	0.48 ± 0.03 (2)	150 ± 0 (2)
26	O-*n*-C_6H_{13}	0.67 ± 0.13 (2)	78 ± 5 (2)
27	O-*n*-C_7H_{15}	4.7 ± 0.3 (3)	410 ± 140 (3)
28	O-*n*-$C_{10}H_{21}$	130 ± 10 (2)	7600 (1)
29	O-*i*-C_3H_7	0.81 ± 0.09 (2)	730 (1)
30	$O(CH_2)_3CH{=}CH_2$	0.33 ± 0.07 (2)	130 ± 30 (2)
31	$O(CH_2)_5OH$	0.95 (1)	880 ± 30 (2)
32	$O(CH_2)_3CN$	6.8 ± 1.7 (2)	5800 ± 200 (2)
96	S-*n*-C_4H_9	0.27 ± 0.02 (2)	100 ± 11 (2)
83	*n*-C_4H_9	0.73 ± 0.03 (2)	610 ± 70 (2)
84	*n*-C_5H_{11}	0.32 ± 0.02 (2)	150 ± 40 (2)
85	*n*-C_6H_{13}	0.62 ± 0.08 (2)	69 ± 1 (2)
86	*i*-C_3H_7	0.63 ± 0.11 (2)	2500 (1)
87	*c*-C_5H_9	0.53 ± 0.08 (2)	350 ± 10 (2)
88	CH_2-*c*-C_6H_{11}	0.58 ± 0.02 (2)	46 ± 2 (2)
89	$(CH_2)_2CH(CH_3)_2$	1.9 ± 0.1 (2)	480 ± 80 (2)
90	$(CH_2)_3OCH_3$	1.8 ± 0 (2)	710 ± 80 (2)
91	$(CH_2)_4OH$	2.3 ± 0.4 (2)	1800 ± 100 (2)
95	Cl	12 ± 1 (2)	7200 (1)
72	C_6H_5	3.0 ± 0.2 (2)	NT[d]
73	2′-$CH_3OC_6H_4$	3.0 ± 0.7 (2)	3500 ± 100 (2)
74	3′-$CH_3OC_6H_4$	1.6 ± 0.6 (2)	470 ± 10 (2)
48	4′-$CH_3OC_6H_4$	0.51 ± 0.04 (2)	180 (1)
92	4′-$CH_3OC_6H_4CH_2$-	0.52 ± 0.19 (2)	85 (1)
98	4′-$CH_3OC_6H_4O$-	0.21 ± 0.03 (2)	58 ± 1 (2)
33	4′-$CH_3OC_6H_4$-$(CH_2)_2O$-	3.0 (1)	200 ± 70 (2)
75	4′-$C_6H_5CH_2OC_6H_4$	6.3 ± 2.0 (2)	600 ± 40 (2)
76	4′-OHC_6H_4	4.1 ± 0.1 (2)	4800 (1)
77	4′-*i*-$C_3H_7C_6H_4$	4.9 ± 0.2 (2)	750 (1)
78	4′-FC_6H_4	8.0 ± 1.0 (2)	NT[d]
60	3′,4′-(−OCH_2O−)-C_6H_3	3.2 ± 0.2 (2)	170 ± 80 (2)
79	5′-methylthiophen-2-yl	1.0 ± 0.6 (2)	1800 (1)

[a−c] See footnote a−c of Table 1. [d] NT = not tested.

a clear correlation between the chain length and the affinity. The optimal number of the carbon atoms is 4−6 (**19**, **25**, and **26**), which corresponds to 6−9 Å in length.

Structurally distinct groups such as linear alkylthio and alkyl (**96** and **83**−**85**), cyclic and branched alkyl (**86**−**88**), as well as different alkoxy (**29** and **30**), which have 3−7 carbon atoms, also are similarly effective for providing subnanomolar affinity. Although substitution with an oxygen- or nitrogen-containing group at the terminal position (**31**, **32**, **90**, and **91**) slightly diminished the activity, their IC_{50} values are still respectable. Interestingly, even chlorine (**95**) gives moderate ET_A receptor binding affinity with the IC_{50} value of 12 nM.

The IC_{50} value of each of the 4-aryl derivatives (**72**−**79**, **48**, **92**, **98**, **33**, and **60**) is consistently lower by an order of 10^2−10^3 than that of the parent compound **82**, showing an order of affinity similar to the above 4-aliphatic series. Similarly to the results in Table 1, the *p*-anisyl group (**48**) was found to be the optimal 4-aryl substituent. Interestingly, insertion of a methylene or oxygen spacer between the *p*-anisyl group and the 4-position (**92** and **98**) showed similar effects on the binding affinity of **48** giving subnanomolar affinities, whereas insertion of a longer ethoxy spacer (**33**) resulted in a loss in the affinity.

All of these results indicate that the hydrophobic substituent at the 4-position plays a crucial role for improving the activity, but its shape is not so important in the receptor recognition. A predominant factor for determining the affinity is only the length of the substituent, and the optimal length is estimated to be 6−9 Å. Presumably, the ET_A receptor recognizes only the length of the 4-substituent but not the shape, and accordingly, various types of groups are acceptable at the 4-position.

One plausible explanation for this observation may be an induced fit[64] of the receptor active site to the 4-substituent, in which ligand-induced conformational changes of the hydrophobic pocket in the receptor may take place to accommodate variously shaped 4-substituents. Therefore, in considering the structural diversity acceptable to the 4-position, this region does not seem to be essential for specific recognition by the ET_A receptor.

(5) Substituent Effect at 3-Position. Replacement of the 3-carboxyl group in the 4-*n*-butyl acid **83** and 4-*p*-anisyl acid **48** by methoxycarbonyl (**99** and **35a**) or carbamoyl (**100** and **101**) led to a significant loss in the binding affinity (Table 5). Compounds **102**−**104**, which contain the tetrazole or acylsulfonamide group as a carboxyl bioisostere, were more active than the esters (**99** and **35a**) and the amides (**100** and **101**) but less potent than the carboxylic acids (**83** and **48**). Obviously, the carboxyl group at the 3-position is an essential functional group. The fact that the acidic compounds are consistently more active than the nonacidic compounds indicates an important role of an acidic proton at this region. Thus, the 3-carboxyl group should act as a hydrogen-bonding donor in the ET_A receptor active site.

(6) Effect of 3,4-Double Bond. Reduction of the C3−C4 olefinic bond generally resulted in loss in the ET_A receptor binding affinity (Table 6). The IC_{50} values of the 3,4-dihydro compounds **106** and **107** were 77 and 1.3 nM, respectively, which are 2−100 times higher than those of the corresponding parent compounds. Thus, the 2*H*-chromene skeleton was found to be the best core structure in our series of compounds.

(7) Effect of Absolute Configuration. Relationships between the absolute configuration at the 2-position and the binding affinity are summarized in Table 7. *R* Isomers are more potent than the corresponding racemates and *S* isomers and are therefore the eutomers. The most potent compound in our series of compounds was (*R*)-**48**, which bound to the ET_A receptor with the IC_{50} value of 0.19 nM and with a 630-fold selectivity over the ET_B receptor.

(8) Pharmacokinetics and Pharmacological Studies of (*R*)-48. On the basis of its excellent binding affinity and selectivity, (*R*)-**48** was chosen for further evaluation. Compound (*R*)-**48** retained the highly potent and selective ET_A binding affinity against the human ET receptors (Table 7). The full details of the other functional and pharmacological studies of (*R*)-**48** had

Table 5. Substitutent Effect at the 3-Position

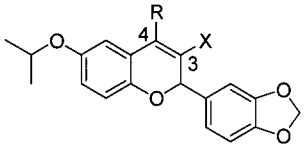

Compd	R	X	IC_{50} (nM)[a] rET_A[b]	IC_{50} (nM)[a] pET_B[c]
83	*n*-C_4H_9	CO_2H	0.73 ± 0.03 (2)	610 ± 70 (2)
99		CO_2Me	>10000 (1)	NT[d]
100		$CONH_2$	410 ± 110 (2)	NT[d]
102			18 ± 4 (2)	NT[d]
103		$CONHSO_2Me$	48 ± 12 (2)	NT[d]
48	4'-$CH_3OC_6H_4$	CO_2H	0.51 ± 0.04 (2)	180 (1)
35a		CO_2Me	>10000 (1)	NT[d]
101		$CONH_2$	630 ± 70 (2)	NT[d]
104		$CONHSO_2Me$	1.8 ± 0.2 (2)	NT[d]

[a–c] See footnotes a–c of Table 1. [d] NT = not tested.

Table 6. Effect of the C3–C4 Double Bond on the Receptor Binding Affinity

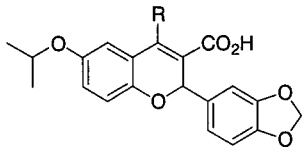

48, 83

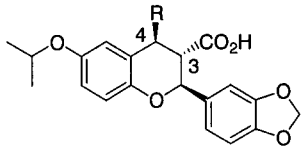

106, 107

Compd	R	IC_{50} (nM)[a] rET_A[b]	IC_{50} (nM)[a] pET_B[c]
83	*n*-C_4H_9	0.73 ± 0.03 (2)	610 ± 70 (2)
106	*n*-C_4H_9	77 ± 7 (2)	NT[d]
48	4'-$CH_3OC_6H_4$	0.51 ± 0.04 (2)	180 (1)
107	4'-$CH_3OC_6H_4$	1.3 (1)	3400 ± 200 (2)

[a–c] See footnotes a–c of Table 1. [d] NT = not tested.

been already reported in our previous report,[65] which demonstrates that this compound is a potent, orally active and long-lasting ET_A receptor antagonist.

Pharmacokinetic studies of (*R*)-**48** were also carried out. The results of intravenous and oral administration in rats are shown in Figure 3. Intravenous administration of (*R*)-**48** gave a terminal-phase half-life of 8.6 ± 0.6 h (mean ± standard deviation), an area under the curve (from time 0 to infinity) of 65.4 ± 14.7 μg h/mL, and a total plasma clearance of 1.3 ± 0.3 mL/min/kg. Orally administrated (*R*)-**48** was rapidly absorbed, and then, the plasma concentration was kept at a high level for more than 8 h. A maximum plasma concentration of 30.6 ± 13.3 μg/mL was achieved at 1.3 ± 0.6 h. Area under the curve (from time 0 to 48 h) was 214 ± 40 μg h/mL. The calculated bioavailability was 54.6 ± 10.2%.

Table 7. ET Receptors Binding Affinities of the Chiral Compounds

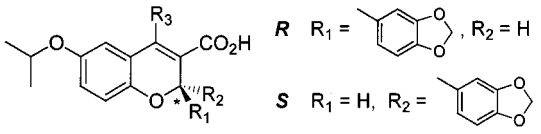

compd	configuration	R_3	IC_{50} (nM)[a] rET_A[b]	IC_{50} (nM)[a] pET_B[c]	B/A[d]
82	*RS*	H	330 ± 30 (2)	52 000 ± 14000 (2) (2)	160
(*R*)-**82**	*R*	H	240 ± 70 (2)	52 000 (1)	220
(*S*)-**82**	*S*	H	1600 (1)	>100 000 (1)	>60
22	*RS*	OCH_3	9.1 ± 0.1 (2)	6400 (1)	700
(*R*)-**22**	*R*	OCH_3	5.2 (1)	3500 ± 1300 (2)	670
83	*RS*	*n*-C_4H_9	0.73 ± 0.03 (2)	610 ± 70 (2)	840
(*R*)-**83**	*R*	*n*-C_4H_9	0.42 ± 0.12 (2)	400 ± 60 (2)	950
48	*RS*	4′-$CH_3OC_6H_4$	0.51 ± 0.04 (2)	180 (1)	350
(*R*)-**48**	*R*	4′-$CH_3OC_6H_4$	0.19 ± 0.01 (2)	120 (1)	630
(*S*-1255)			(0.45 (1))[e]	(200 (1))[e]	(440)[e]
(*S*)-**48**	*S*	4′-$CH_3OC_6H_4$	15 ± 3 (2)	1500 (1)	100

[a–c] See footnotes a–c of Table 1. [d] IC_{50} (ET_B)/IC_{50} (ET_A). [e] Human ET_A and ET_B receptors.

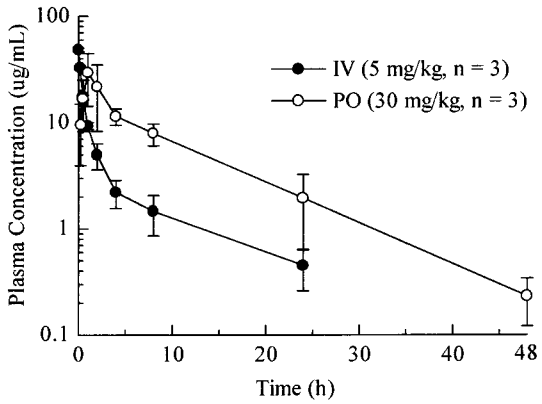

Figure 3. Pharmacokinetics of (*R*)-**48** in rats.

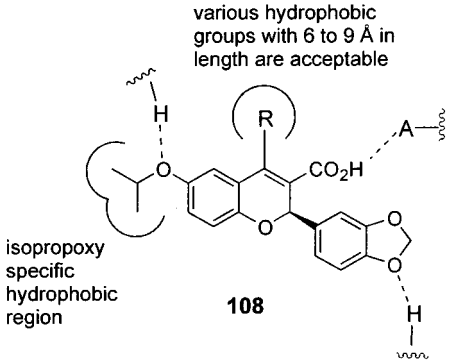

Figure 4. Crucial basic structure **108** of our ET_A receptor antagonists and its speculated pharmacophore model. H and A indicate a hydrogen and a hydrogen bonding acceptor on the receptor active sites, respectively.

With these preferable pharmacokinetic and pharmacological profiles, (*R*)-**48** was selected as our clinical candidate.

Conclusion

A unique lead compound **3** was found by screening our AII receptor antagonists, and the subsequent optimization led us to the discovery of the compounds with highly potent binding affinity for the ET_A receptor, of which (*R*)-**48** was selected as a clinical candidate.

Extensive chemical modifications of **3** also revealed the crucial roles of the substituents at the 2-, 3-, 6-, and 4-positions on the (*R*)-2*H*-chromene skeleton for binding affinity. These four substituents are equally indispensable for potent binding affinity, but their roles in the receptor recognition seem to be significantly different. Substitutions of the 2-, 3-, and 6-positions with the *m*,*p*-methylenedioxyphenyl group, the carbonyl group, and the isopropoxy group, respectively, are essential for improving high potency, and consequently these groups are recognized by the ET_A receptor. They potentially act as a hydrogen bond acceptor or donor in the receptor active site and are considered to play predominant roles in the receptor recognition. In contrast to these positions, introduction of various aliphatic and aromatic substituents, 6–9 Å in length, at the 4-position retains the high potency, thereby suggesting that this region is not essential for the specific receptor recognition. These SAR studies led to the conclusion that substructure **108** (Figure 4) is a crucial basic structure of our ET_A receptor antagonists and is specifically recognized by the ET_A receptor through three hydrogen bonds, whereas the substituent at the 4-position plays a pivotal role to help **108** guide into the relevant position of the receptor active site. This conclusion is illustrated in a pharmacophore model in Figure 3.

Experimental Section

Melting points were determined on a Yanagimoto hot plate apparatus and are uncorrected. ^1H NMR spectra were recorded on a Varian VXR-300 spectrometer and are reported in parts per million (δ) relative to tetramethylsilane (TMS) as an internal standard. Optical rotations were measured in a 10 cm cell on a Perkin-Elmer 241 polarimater. Column chromatography was performed using a column packed with Merck silica gel 60 (70–230 mesh). Analytical HPLC was performed on a Shimadzu LC-10AD instrument.

5-Isopropoxy-2-hydroxyacetophenone (5a). A mixture of 2,5-dihydroxyacetophenone **4a** (7.61 g, 50.02 mmol), 2-bromopropane (18.46 g, 150.09 mmol), sodium iodide (1.50 g, 10.01 mmol), powdered potassium carbonate (8.29 g, 59.98 mmol), and DMF (30 mL) was stirred at 60 °C for 24 h. The mixture was poured into water and extracted with ethyl acetate. The combined organic extracts were washed with water and brine, dried with $MgSO_4$, and concentrated. The residue was purified by column chromatography on silica gel (ethyl acetate/hexane, 1/19) to give **5a** as a yellow oil (4.98 g, 51.3%). ^1H NMR ($CDCl_3$): δ 1.32 (6H, d, J = 6.1 Hz), 2.60 (3H, s), 4.34–4.52 (1H, m), 6.89–7.23 (3H, m).

6-Isopropoxy-4-oxo-4*H*-chromene-3-carbaldehyde (6) (R_1 = 6-Isopropoxy). Phosphoryl oxychloride (388 g, 2.54 mol) was added dropwise to **5a** (123 g, 0.634 mol) in DMF (800 mL) at −30 °C. The mixture was allowed to stand overnight at room temperature and then poured into ice-water. The resulting precipitate was collected by filtration, giving **6** (119 g, 81%) as a dark brown solid. ^{1}H NMR ($CDCl_3$): δ 1.39 (6H, d, J = 6.0 Hz), 4.71 (1H, m), 7.28 (1H, dd, J = 9.4 and 2.6 Hz), 7.46 (1H, d, J = 9.4 Hz), 7.64 (1H, d, J = 2.6 Hz), 8.53 (1H, s), 10.40 (1H, s).

6-Isopropoxy-4-oxo-4*H*-chromene-3-carboxylic Acid (7) (R_1 = 6-Isopropoxy). A solution of sodium chlorite (80%, 77 g, 0.684 mol) in water (400 mL) was added dropwise to a mixture of **6** (R_1 = 6-isopropoxy, 40.0 g, 0.172 mol) in dichloromethane (860 mL) and NH_2SO_3H (84.0 g, 0.865 mol) in water (840 mL) at 0 °C. After 30 min, the organic layer was separated and the aqueous layer was extracted with chloroform. The combined organic phases were washed with water and brine, dried with $MgSO_4$, and concentrated. Recrystallization from ethanol afforded **7** (34.8 g, 82%) as yellow crystals; mp 178 °C. ^{1}H NMR ($CDCl_3$): δ 1.41 (6H, d, J = 6.0 Hz), 4.72 (1H, m), 7.39 (1H, dd, J = 9.2 and 3.0 Hz), 7.58 (1H, d, J = 9.2 Hz), 7.62 (1H, d, J = 3.2 Hz), 8.99 (1H, s), 13.6 (1H, brs).

Methyl 6-Isopropoxy-4-oxo-4*H*-chromene-3-carboxylate (8) (R_1 = 6-Isopropoxy). Oxalyl chloride (20.4 g, 0.16 mol) was added dropwise to a solution of **7** (R_1 = 6-isopropoxy, 34.8 g, 0.14 mol) and DMF (2.0 mL, 0.026 mol) in dichloromethane (350 mL) at room temperature. After 1 h, methanol (30 mL) was carefully added, and the mixture was stirred for 15 min. The solvent was removed under reduced pressure, and the residue was recrystallized from ethanol to give **8** (36.3 g, 99%) as colorless needles; mp 124−126 °C. ^{1}H NMR ($CDCl_3$): δ 1.37 (6H, d, J = 6.0 Hz), 3.93 (3H, s), 4.69 (1H, m), 7.24 (1H, dd, J = 9.0 and 3.0 Hz), 7.42 (1H, d, J = 9.0 Hz), 7.63 (1H, d, J = 3.0 Hz), 8.66 (1H, s).

Methyl 2-(Benzo[1,3]dioxol-5-yl)-6-isopropoxy-4-oxochromane-3-carboxylate (9) (R_1 = 6-Isopropoxy, R_2 = *m*,*p*-Methylenedioxyphenyl). 1,2-Dibromoethane (634 mg, 3.37 mmol) was added to magnesium turnings (1.72 g, 70.86 mmol) in tetrahydrofuran (THF, 10 mL), and the mixture was stirred for 10 min at room temperature. A solution of 4-bromo-1,2-methylenedioxybenzene (13.57 g, 67.49 mmol) in THF (100 mL) was added dropwise, and the mixture was refluxed for 1 h to complete the reaction. The mixture was cooled to room temperature, and copper(I) iodide (479 mg, 2.52 mmol) was added. The mixture was stirred for 15 min and then cooled to 0 °C, and then, a solution of **8** (R_1 = 6-isopropoxy, 10.0 g, 38.13 mmol) in THF (100 mL) was added dropwise. After it was stirred at 0 °C for 1 h, the reaction mixture was poured into ice-water and 1 M HCl (75 mL) was added. Ether extraction followed by silica gel chromatography (toluene/acetonitrile, 95/5) afforded a mixture of keto−enol isomers of **9** (13.6 g, 93%) as a yellow oil. ^{1}H NMR ($CDCl_3$): δ 1.30 (6H, d, J = 6.3 Hz, CH_3, enol), 1.32 (6H, d, J = 6.3 Hz, CH_3, keto), 3.68 (3H, s, CO_2CH_3, keto), 3.76 (3H, s, CO_2CH_3, enol), 4.02 (1H, d, J = 12.3 Hz, $C_{(3)}$H, keto), 4.42−4.50 (1H, m, CH, enol), 4.48−4.56 (1H, m, CH, keto), 5.55 (1H, d, J = 12.3 Hz, $C_{(2)}$H, keto), 5.91-(2H, s, −OCH_2O-, enol), 6.00 (2H, s, −OCH_2O-, keto), 6.10 (1H, s, $C_{(2)}$H, enol), 6.68−7.36 (12H, m, arom, keto and enol).

Methyl 2-(Benzo[1,3]dioxol-5-yl)-4-*n*-butyloxyl-6-isopropoxy-2*H*-chromene-3-carboxylate (10) (R_1 = 6-Isopropoxy, R_2 = *m*,*p*-Methylenedioxyphenyl, R_3 = *n*-Butyl). A solution of diethyl azodicarboxylate (136 mg, 0.780 mmol) in THF (2 mL) was added dropwise to a stirred solution of **9** (R_1 = 6-isopropoxy, R_2 = *m*,*p*-methylenedioxyphenyl, 200 mg, 0.520 mmol), triphenylphosphine (205 mg, 0.780 mmol), and *n*-butanol (58 mg, 0.780 mol) in THF (2 mL) at −10 °C. The stirring was continued for 3 h at −10 °C, and the reaction was quenched by addition of water. After usual workup, the product was purified by column chromatography on silica gel (ethyl acetate/hexane, 1/4), giving **10** (211 mg, 92%) as a pale yellow oil. ^{1}H NMR ($CDCl_3$): δ 1.00 (3H, t, J = 7.4 Hz), 1.30 (6H, d, J = 6.4 Hz), 1.52 (2H, m), 1.84 (2H, m), 3.76 (3H, s), 3.94−4.18 (2H, m), 4.40 (1H, m), 5.89 (2H, s), 6.17 (1H, s), 6.65−6.87 (5H, m,), 7.02 (1H, d, J = 2.8 Hz).

2-(Benzo[1,3]dioxol-5-yl)-4-*n*-butyloxy-6-isopropoxy-2*H*-chromene-3-carboxylic Acid (19). A mixture of **10** (R_1 = 6-isopropoxy, R_2 = *m*,*p*-methylenedioxyphenyl, R_3 = *n*-butyl, 211 mg, 0.479 mmol), 1 M NaOH (2.4 mL), methanol (2.5 mL), and THF (5 mL) was refluxed for 3 h and then concentrated under reduced pressure. After water was added, the mixture was acidified with 1 M HCl and extracted with ether. The product was recrystallized from diisopropyl ether/acetone to give **19** (183 mg, 90%) as yellow crystals; mp 124−125 °C. ^{1}H NMR ($CDCl_3$): δ 1.01 (3H, t, J = 7.4 Hz), 1.32 (6H, d, J = 6.0 Hz), 1.52 (2H, m), 1.88 (2H, m), 3.94−4.06 (1H, m), 4.26−4.47 (2H, m), 5.89 (2H, s), 6.27 (1H, s), 6.67 (1H, d, J = 3.8 Hz), 6.78−6.87 (5H, m). Anal. ($C_{24}H_{26}O_7$) C, H.

Methyl 2-(Benzo[1,3]dioxol-5-yl)-6-isopropoxy-4-(trifluoromethansulfonyloxy)-2*H*-chromene-3-carboxylate (34) (R_1 = 6-Isopropoxy, R_2 = *m*,*p*-Methylenedioxyphenyl). A solution of **9** (R_1 = 6-isopropoxy, R_2 = *m*,*p*-methylenedioxyphenyl, 47.5 g, 0.124 mol) in DMF (100 mL) was added dropwise to sodium hydride (3.60 g, 0.150 mol) in DMF (400 mL) at 0 °C, and the mixture was stirred for 1 h. 2-[*N*,*N*′-Bis-(trifluoromethansulfonyl)amino]pyridine (50.8 g, 0.142 mol) was added, and the mixture was stirred at 0 °C for 3 h and then poured into ice-water. Usual workup and purification by silica gel chromatography (toluene) afforded **34** (63.0 g, 99%) as pale yellow crystals; mp 88−90 °C. ^{1}H NMR ($CDCl_3$): δ 1.31 (3H, d, J = 6.4 Hz), 1.31 (3H, d, J = 6.0 Hz), 3.83 (3H, s), 4.40 (1H, m), 5.92 (2H, s), 6.32 (1H, s), 6.68−6.92 (6H, m). Anal. ($C_{22}H_{19}O_9SF_3$) C, H, S, F.

Methyl 2-(Benzo[1,3]dioxol-5-yl)-6-isopropoxy-4-(4-methoxyphenyl)-2*H*-chromene-3-carboxylate (35a). A mixture of **34** (R_1 = 6-isopropoxy, R_2 = *m*,*p*-methylenedioxyphenyl, 37.5 g, 72.6 mmol), aqueous sodium carbonate (2M, 102 mL, 204 mmol), lithium chloride (9.2 g, 217 mmol), $Pd(Ph_3P)_4$ (1.68 g, 1.45 mmol), 4-methoxyphenylboronic acid (12.1 g, 79.6 mmol), and dimethoxyethane (400 mL) was refluxed for 3 h. After water was added, the mixture was extracted with ether. The product was purified by column chromatography on silica gel (ethyl acetate/hexane, 1/4) to give **35a** (32.4 g, 94%) as a pale yellow oil. ^{1}H NMR ($CDCl_3$): δ 1.18 (3H, t, J = 6.0 Hz), 1.19 (3H, d, J = 6.0 Hz), 3.48 (3H, s), 3.87 (3H, s), 4.21 (1H, m), 5.92 (2H, s), 6.18 (1H, s), 6.30 (1H, m), 6.71−7.21 (9H, m). Anal. ($C_{28}H_{26}O_7$) C, H.

2-(Benzo[1,3]dioxol-5-yl)-6-isopropoxy-4-(4-methoxyphenyl)-2*H*-chromene-3-carboxylic Acid (48). Acid **48** was prepared from **35a** in a manner similar to that used for the synthesis of **19** (66%). Yellow crystals; mp 179−181 °C. ^{1}H NMR ($CDCl_3$): δ 1.15 (3H, d, J = 6.0 Hz), 1.18 (3H, d, J = 6.0 Hz), 3.87(3H, s), 4.19 (1H, m), 5.91 (2H, s), 6.15 (1H, s), 6.25-(1H, m), 6.69−6.74(3H, m), 6.87−6.97 (4H, m), 7.15−7.19(2H, br). Anal. ($C_{27}H_{24}O_7$) C, H.

2-(Benzo[1,3]dioxol-5-yl)-6-isopropoxy-2*H*-chromene-3-carboxylic Acid (82). Ester **9** (R_1 = 6-isopropoxy, R_2 = *m*,*p*-methylenedioxyphenyl, 1.51 g, 3.93 mmol) was hydrogenated over 10% Pd/C (200 mg) in ethyl acetate (12 mL) for 30 min. The catalyst was removed by filtration, and the filtrate was concentrated to give **80** (R_1 = 6-isopropoxy, R_2 = *m*,*p*-methylenedioxyphenyl, 1.10 g, 72%). A solution of **80** and *p*-toluenesulfonic acid monohydrate (260 mg, 1.37 mmol) in toluene (50 mL) was refluxed for 1 h. The reaction mixture was washed with aqueous $NaHCO_3$ and brine, dried with $MgSO_4$, and then concentrated. The residue was purified by silica gel chromatography (ethyl acetate/hexane, 1/4) to afford **81** (R_1 = 6-isopropoxy, R_2 = *m*,*p*-methylenedioxyphenyl, 1.00 g, 69%). Ester **81** was hydrolyzed in a similar manner as described for the synthesis of **19** to give **82** (800 mg, 57% from **9**) as yellow crystals; mp 159−161 °C. ^{1}H NMR ($CDCl_3$): δ 1.30 (6H, d, J = 6.3 Hz), 4.40 (1H, m), 5.90 (2H, s), 6.10 (1H, s), 6.68−6.85 (6H, m), 7.71 (1H, s). Anal. ($C_{20}H_{18}O_6$) C, H.

2-(Benzo[1,3]dioxol-5-yl)-4-*n*-butyl-6-isopropoxy-2*H*-chromene-3-carboxylic Acid (83). 4-Methoxy acid **22** was synthesized as described for the synthesis of **19**. A solution of **22** (192 mg, 0.499 mmol) in THF (2.5 mL) was added dropwise

to *n*-butylmagnesium chloride (2.0 M solution in ether, 1.3 mL, 2.60 mmol) at −35 °C. After it was stirred for 1 h at −35 °C and at 0 °C for 2 h, the mixture was poured into acetic acid (0.15 mL, 2.64 mmol) in ice-water and extracted with ethyl acetate. The product was purified by column chromatography on silica gel (ethyl acetate/hexane, gradient from 1/4 to 1/2) to give **83** (161 mg, 79%) as yellow crystals; mp 140−141 °C. ^{1}H NMR ($CDCl_3$): δ 0.98 (3H, t, J = 6.8 Hz), 1.30 (3H, d, J = 6.0 Hz), 1.31 (3H, d, J = 6.0 Hz), 1.38−1.74 (4H, m), 3.08 (2H, m), 4.40 (1H, m), 5.89 (2H, s), 6.13 (1H, s), 6.66 (1H, d, J = 7.8 Hz), 6.73−6.85 (3H, m), 6.74 (1H, d, J = 7.8 Hz), 6.96 (1H, d, J = 2.2 Hz). Anal. ($C_{24}H_{26}O_6$) C, H.

2-(Benzo[1,3]dioxol-5-yl)-6-isopropoxychroman-4-one (93). A solution of **5a** (219 g, 1.13 mol), piperonal (170 g, 1.13 mol), and 2 M NaOH (1.13 L) in methanol (570 mL) was stirred at room temperature for 3 days. The resulting precipitate was collected to give **93** as yellow crystals (336 g, 91%); mp 125−126 °C. ^{1}H NMR ($CDCl_3$): δ 1.33 (6H, d, J = 6.1 Hz), 2.76−3.11 (2H, m), 4.44−4.62 (1H, m), 5.34 (1H, dd, J = 3.2 and 13.0 Hz), 5.99 (2H, s), 6.81−7.36 (6H, m).

2-(Benzo[1,3]dioxol-5-yl)-4-chloro-6-isopropoxy-2*H*-chromene-3-carbaldehyde (94). Phosphoryl oxychloride (6.09 g, 39.7 mmol) was added to DMF (12 mL) at 0 °C. After 30 min, a solution of **93** (5.19 g, 15.9 mmol) in DMF (20 mL) was added dropwise thereto at 0 °C, and then, the mixture was stirred at room temperature for 2 days. The reaction mixture was poured into ice-water and extracted with ethyl acetate. The product was purified by silica gel chromatography (toluene) followed by recrystallization (diisopropyl ether/acetone) to afford **94** (4.83 g, 82%) as yellow crystals; mp 126−127 °C. ^{1}H NMR ($CDCl_3$): δ 1.33 (6H, d, J = 6.0 Hz), 4.38−4.57 (1H, m), 5.90 (2H, s), 6.23 (1H, s), 6.60−7.26 (6H, m), 10.26 (1H, s).

2-(Benzo[1,3]dioxol-5-yl)-4-chloro-6-isopropoxy-2*H*-chromene-3-carboxylic Acid (95). A solution of **94** (92.0 g, 247 mmol) in toluene (1.38 L) was added to NH_2SO_3H (57.6 g, 593 mmol) in water (346 mL). After the mixture was cooled to 0 °C, a solution of sodium chlorite (80%, 56.0 g, 495 mmol) in water (346 mL) was added dropwise, and the mixture was stirred for 20 min. Aqueous solution of sodium sulfite (31.0 g in 100 mL water, 246 mmol) and aqueous NaOH (40.0 g in 700 mL water) were successively added to the reaction mixture. The aqueous layer was separated and acidified with 37% HCl. The resulting precipitate was collected by filtration to give **95** (87.5 g, 91%) as yellow crystals; mp 177 °C. ^{1}H NMR ($CDCl_3$) δ: 1.31 (6H, d, J = 6.0 Hz), 4.45 (1H, m), 5.90 (2H, s), 6.24 (1H, s), 6.66−6.85 (5H, m), 7.23−7.26 (1H, m). Anal. ($C_{20}H_{17}ClO_6$) C, H, Cl.

2-(Benzo[1,3]dioxol-5-yl)-4-butylsulfanyl-6-isopropoxy-2*H*-chromene-3-carboxylic Acid (96). A solution of 1-butanethiol (108 mg, 1.20 mmol) in THF (1 mL) was added to sodium hydride (60%, 84 mg, 2.10 mmol) in THF (1 mL) at room temperature. The mixture was stirred for 30 min, and then, a solution of **95** (382 mg, 0.982 mmol) in THF (6 mL) was added at 0 °C. After it was stirred for 30 min at 0 °C, the reaction was quenched by addition of acetic acid (0.2 mL) and the mixture was extracted with ethyl acetate. The usual workup and purification by silica gel column chromatography (ethyl acetate/hexane, gradient from 1/9 to 1/4), followed by recrystallization from 2-propanol/hexane afforded **96** (33 mg, 15%) as yellow crystals; mp 138−142 °C. ^{1}H NMR ($CDCl_3$): δ 0.88 (3H, t, J = 7.2 Hz), 1.17−1.69 (4H, m), 1.31 (3H, d, J = 6.0, Hz), 1.32 (3H, d, J = 6.0 Hz), 2.83 (2H, t, J = 7.4 Hz), 4.44 (1H, m), 5.89 (2H, s), 6.37 (1H, s), 6.64 (1H, d, J = 6.0 Hz), 6.72 (1H, dd, J = 0.6 and 1.6 Hz), 6.73−6.87 (3H, m), 7.27 (1H, m). Anal. ($C_{24}H_{26}O_6S$) C, H, S.

2-(Benzo[1,3]dioxol-5-yl)-6-isopropoxy-4-(4-methoxyphenoxy)-2*H*-chromene-3-carbaldehyde (97). A solution of 4-methoxyphenol (366 mg, 2.95 mmol) in THF (4 mL) was added dropwise to sodium hydride (60%, 134 mg, 3.35 mmol) in THF (2 mL) at room temperature. After it was stirred for 1 h, a solution of **94** (500 mg, 1.34 mmol) in THF (5 mL) was added dropwise. The mixture was stirred for 6 h at room temperature and then poured into ice-water. After extraction with ether and purification by silica gel chromatography (toluene/ethyl acetate, 9/1), the product was recrystallized from diisopropyl ether/acetone to give **97** (480 mg, 78%) as yellow crystals; mp 94−95 °C. ^{1}H NMR: δ 1.05 (3H, d, J = 6.0 Hz), 1.19 (3H, d, J = 6.0 Hz), 3.75 (3H, s), 4.14−4.23 (1H, m), 5.89 (2H, s), 6.32 (1H, s), 6.69 (2H, d, J = 8.1 Hz), 6.80−6.88 (6H, m), 6.98 (2H, d, J = 9.0 Hz), 10.09 (1H, s). Anal. ($C_{27}H_{24}O_7$) C, H.

2-(Benzo[1,3]dioxol-5-yl)-6-isopropoxy-4-(4-methoxyphenoxy)-2*H*-chromene-3-carboxylic Acid (98). A solution of sodium chlorite (80%, 130 mg, 1.15 mmol) in water (1 mL) was added to a mixture of aldehyde **97** (100 mg, 0.217 mmol) in dimethyl sulfoxide (DMSO, 7 mL) and $NaH_2PO_4{\cdot}2H_2O$ (64 mg, 0.412 mmol) in water (1 mL) at room temperature. After it was stirred for 20 h, the reaction mixture was diluted with water, extracted with ethyl acetate, and recrystallized from ethyl acetate/hexane to afford **98** (148 mg, 82%) as yellow crystals; mp 188−190 °C. ^{1}H NMR ($CDCl_3$ + CD_3OD): δ 1.06 (3H, d, J = 6.0 Hz), 1.19 (3H, d, J = 6.0 Hz), 3.75 (3H, s), 4.11−4.29 (1H, m), 5.92 (2H, s), 6.30 (1H, s), 6.69−6.97 (10H, m). Anal. ($C_{27}H_{24}O_8$) C, H.

Methyl 2-(Benzo[1,3]dioxol-5-yl)-4-*n*-butyl-6-isopropoxy-2*H*-chromene-3-carboxylate (99). Oxalyl chloride (78 μL, 0.877 mmol) was added dropwise to a solution of **83** (300 mg, 0.731 mmol) and DMF (15 μL) in CH_2Cl_2 (2.5 mL) at room temperature. After it was stirred at room temperature for 20 min, methanol (2 mL) was added. After 5 min, water was added and the mixture was extracted with ethyl acetate. Usual workup followed by column chromatography on silica gel (ethyl acetate/hexane, 1/5) gave **99** (190 mg, 83%) as a yellow oil. ^{1}H NMR ($CDCl_3$): δ 0.99 (3H, t, J = 7.4 Hz), 1.30 (3H, d, J = 6.0 Hz), 1.31 (3H, t, J = 6.0 Hz), 1.43−1.69 (4H, m), 2.96−3.08 (2H, m), 3.72 (3H, s), 4.26−4.44 (1H, m), 5.90 (2H, s), 6.11 (1H, s), 6.65−6.82 (5H, m), 6.95 (1H, d, J = 2.4 Hz). Anal. ($C_{25}H_{28}O_6{\cdot}0.15H_2O$) C, H.

2-(Benzo[1,3]dioxol-5-yl)-4-*n*-butyl-6-isopropoxy-2*H*-chromene-3-carboxamide (100). Oxalyl chloride (78 μL, 0.877 mmol) was added dropwise to a solution of **83** (300 mg, 0.731 mmol) and DMF (15 μL) in CH_2Cl_2 (3 mL) at room temperature. After it was stirred at room temperature for 1 h, the mixture was mixed with 28% NH_4OH (3 mL) and then extracted with ethyl acetate. Usual workup and column chromatography on silica gel (chloroform/acetonitrile, 95/5) followed by recrystallization from isopropyl ether/acetone gave **100** (231 mg, 77%) as colorless crystals; mp 115−116 °C. ^{1}H NMR ($CDCl_3$): δ 0.96 (3H, d, J = 7.2 Hz), 1.31 (3H, d, J = 6.3 Hz), 1.32 (3H, d, J = 6.3 Hz), 1.42−1.63 (4H, m), 2.70−2.88 (2H, m), 4.35−4.49 (1H, m), 5.40 (2H, br), 5.83 (1H, s), 5.92 (2H, s), 6.66−6.73 (3H, m), 6.86−6.88 (3H, m). Anal. ($C_{24}H_{27}NO_5$) C, H, N.

2-(Benzo[1,3]dioxol-5-yl)-4-*n*-butyl-6-isopropoxy-2*H*-chromene-3-tetrazole (102). A mixture of **100** (100 mg, 0.244 mmol), sodium azide (238 mg, 3.66 mmol), tetrachlorosilane (140 μL, 1.22 mmol), and acetonitrile (4 mL) was refluxed for 16 h. The reaction was quenched with 2 M Na_2CO_3, and the mixture was extracted with ethyl acetate. Usual workup and purification by column chromatography on silica gel (chloroform/acetonitrile, 95/5) afforded **102** (65 mg, 61%) as a light brown oil. ^{1}H NMR ($CDCl_3$): δ 0.96 (3H, t, J = 7.3 Hz), 1.33 (3H, d, J = 6.0 Hz), 1.34 (3H, d, J = 6.0 Hz), 1.42−1.55 (2H, m), 1.62−1.73 (2H, m), 2.93−3.10(2H, m), 4.40−4.48 (1H, m), 5.90 (2H, s), 6.15 (1H, s), 6.66−6.85 (5H, m), 6.98−6.99 (1H, m). Anal. ($C_{24}H_{26}N_4O_4{\cdot}0.3H_2O$) C, H, N.

***N*-[2-(Benzo[1,3]dioxol-5-yl)-4-*n*-butyl-6-isopropoxy-2*H*-chromene-3-carbonyl]methanesulfonamide (103).** A solution of **83** (100 mg, 0.244 mmol), methanesulfonamide (25 mg, 0.268 mmol), 1-ethyl-3-[3-(dimethylamino)propyl]carbodiimide hydrochloride (51 mg, 0.268 mmol), and 4-(dimethylamino)pyridine (33 mg, 0.268 mmol) in THF (2 mL) and CH_2Cl_2 (4 mL) was stirred for 16 h. Water was added, and the mixture was extracted with ethyl acetate. The product was purified by column chromatography on silica gel (ethyl acetate/hexane, 1/1) to give **103** (65 mg, 55%) as a yellow oil. ^{1}H NMR ($CDCl_3$): δ 0.94 (3H, t, J = 7.1 Hz), 1.30 (3H, d, J = 6.0 Hz),

1.31 (3H, d, J = 6.0 Hz), 1.40−1.50 (2H, m), 1.54−1.64 (2H, m), 2.77−2.97 (2H, m), 3.04 (3H, s), 4.36−4.44 (1H, m), 5.87 (2H, s), 5.91 (1H, s), 6.65−6.71 (3H, m), 6.82−6.89 (3H, m). Anal. ($C_{25}H_{29}NO_7S\cdot 1.0H_2O$) C, H, N, S.

Methyl 2-(Benzo[1,3]dioxol-5-yl)-6-isopropoxy-4-(4-methoxyphenyl)-chromane-3-carboxylate (105b). A mixture of **35a** (1.50 g, 3.15 mmol), palladium chloride (2.01 g, 11.34 mmol), methanol (30 mL), and CH_2Cl_2 (10 mL) was stirred under 500 kPa of hydrogen pressure for 72 h. The catalyst was removed by filtration, and the filtrate was concentrated under reduced pressure. The precipitate was triturated with isopropyl ether to give **105b** (667 mg, 45%). ^{1}H NMR ($CDCl_3$): δ 1.21 (3H, d, J = 6.2 Hz), 1.24 (3H, d, J = 6.2 Hz), 3.21 (3H, s), 3.27 (1H, dd, J = 2.6 and 6.5 Hz), 3.80 (3H, s), 4.24−4.33 (1H, m), 4.63 (1H, d, J = 6.5 Hz), 5.27 (1H, d, J = 2.6 Hz), 5.96 (2H, s), 6.47−6.48 (1H, m), 6.74−6.95 (7H, m), 7.14 (2H, d, J = 8.7 Hz).

2-(Benzo[1,3]dioxol-5-yl)-6-isopropoxy-4-(4-methoxyphenyl)-chromane-3-carboxylic Acid (107). Acid **107** (53% yield) was synthesized from **105b** in a manner similar to that used for synthesis of **19**. Colorless crystals; mp 272 °C (dec). ^{1}H NMR ($CDCl_3$ + CD_3OD): 1.17 (3H, d, J = 6.0 Hz), 1.22 (3H, d, J = 6.3 Hz), 3.09 (1H, dd, J = 9.9 and 11.4 Hz), 3.80 (3H, s), 4.26 (1H, m), 4.50 (1H, d, J = 11.4 Hz), 5.05 (1H, d, J = 9.9 Hz), 5.96 (2H, s), 6.30 (1H, br), 6.70−7.00 (7H, m), 7.13 (2H, d, J = 8.4 Hz). Anal. ($C_{27}H_{26}O_7\cdot 0.1H_2O$) C, H.

Preparation of Chiral Compounds (*R*)-48 and (*S*)-48. A solution of **48** (20.0 g, 43.4 mmol) and (1*S*,2*R*)-(+)-norephedrine (6.56 g, 43.4 mmol) in acetonitrile (40 mL) was allowed to stand overnight at room temperature. The precipitate was recrystallized successively from 2-propanol and ethanol to give the salt (7.8 g, 30%, 99% ee). A solution of the salt in water was treated with 1 M HCl (12.8 mL) and extracted with ethyl acetate. The acid was recrystallized from 2-propanol to give (*R*)-**48** (5.03 g, 25%, 100% ee) as pale yellow crystals; mp 170−171 °C. $[\alpha]_D^{24}$ +178.8 (c 1.00, CH_3OH). ^{1}H NMR($CDCl_3$): δ 1.15 (3H, d, J = 5.8 Hz), 1.18 (3H, d, J = 5.8 Hz), 3.88 (3H, s), 4.19 (1H, m), 5.91 (2H, s), 6.16 (1H, s), 6.25 (1H, m), 6.69−6.74 (3H, m), 6.90−6.97 (4H, m), 7.16−7.19 (2H, m). Anal. ($C_{27}H_{24}O_7$) C, H. The enantiomeric purity of (*R*)-**48** was determined by HPLC: column, CHIRALCEL OJ-R (4.6 mm × 150 mm, DAICEL); solvent, acetonitrile/H_2O/trifluoroaceti acid = 68/31/0.1; flow rate, 0.5 mL/min, detection, 286 nm: t_R = 6.1 min.

In a similar manner, (*S*)-**48** was obtained via the (1*R*,2*S*)-(−)-norephedrine salt (28%, 100% ee); mp 170−171 °C. $[\alpha]_D^{24}$ −177.3 (c 1.00, CH_3OH). Anal. ($C_{27}H_{24}O_7$) C, H. HPLC: t_R = 12.4 min; 100%ee.

(*R*)-22. Acid (*R*)-**22** was obtained in a manner similar to that used for preparation of (*R*)-**48**, except that acetonitrile was replaced by methanol (37%, 99.7% ee); mp 136−137 °C. $[\alpha]_D^{24}$ +42.6 (c 1.00, CH_3OH). ^{1}H NMR ($CDCl_3$): δ 1.30 (3H, d, J = 6.0 Hz), 1.31 (3H, d, J = 6.0 Hz), 4.01 (3H, s), 4.43(1H, m), 5.89 (2H, s), 6.25 (1H, s), 6.65−6.92 (6H, m). Anal. ($C_{21}H_{20}O_7$) C, H. The enantiomeric purity was determined by HPLC: column, CHIRALCEL OJ-R (4.6 mm × 150 mm, DAICEL); solvent, acetonitrile/0.2 M H_3PO_4−KH_2PO_4 = 50/50; flow rate, 0.5 mL/min; detection, 286 nm; t_R = 10.1 min.

(*R*)-82 and (*S*)-82. Acid **82** (800 mg, 2.26 mmol) was treated with (*R*)-(+)-phenylethylamine (274 mg, 2.26 mmol) in methanol. The precipitate was collected and recrystallized repeatedly from methanol to give the salt (99.5% ee). Acid hydrolysis and recrystallization from ethanol gave (*S*)-**82** (200 mg, 25%, 98%ee) as yellow needles; mp 151.5−152 °C. $[\alpha]_D^{28}$ +6.6 (c 1.01, CH_3OH). ^{1}H NMR ($CDCl_3$): δ 1.30 (6H, d, J = 6.3 Hz), 4.40 (1H, m), 5.90 (2H, s), 6.10 (1H, s), 6.68−6.85 (6H, m), 7.71 (1H, s). Anal. ($C_{20}H_{18}O_6$) C, H. The enantiomeric purity was determined by HPLC: column, CHIRALCEL OJ-R (4.6 mm × 150 mm, DAICEL); solvent, acetonitrile/H_2O/trifluoroaceti acid = 70/30/0.1; flow rate, 0.5 mL/min; detection, 286 nm; t_R = 5.5 min.

In a similar manner, (*R*)-**82** was obtained via the (*S*)-(−)-phenylethylamine salt (23%, 99% ee); mp 151−152 °C. $[\alpha]_D^{28}$ −7.3 (c 1.01, CH_3OH). Anal. ($C_{20}H_{18}O_6$) C, H. HPLC: t_R = 7.1 min.

(*R*)-83. Acid (*R*)-**83** was synthesized from (*R*)-**22** in a manner similar to that described for the synthesis of the racemate (89%, 100% ee); mp 148−149 °C. $[\alpha]_D^{23}$ +61.3 (c 1.01, MeOH). ^{1}H NMR ($CDCl_3$): δ 0.98 (3H, t, J = 7.2 Hz), 1.30 (3H, d, J = 6.0 Hz), 1.31 (3H, d, J = 6.0 Hz), 1.38−1.73 (4H, m), 2.92−3.22 (2H, m), 4.40 (1H, m), 5.89 (2H, s), 6.13 (1H, s), 6.66 (1H, d, J = 7.8 Hz), 6.70−6.86 (4H, m), 6.96 (1H, d, J = 2.2 Hz). Anal. ($C_{24}H_{26}O_6$) C, H. The enantiomeric purity was determined by HPLC: column, CHIRALCEL OJ-R (4.6 mm × 150 mm, DAICEL); solvent, acetonitrile/0.5 M $NaClO_4$−$HClO_4$ = 60/40; flow rate, 1.0 mL/min; detection, 286 nm; t_R = 10.1 min.

Single-Crystal X-ray Analysis of (1*S*,2*R*)-(+)-Norephedrine Salt of (*R*)-48. Colorless prismatic crystals of the salt $C_{36}H_{37}O_8$ were grown from methanol solution. A single crystal with approximate dimensions 0.20 mm × 0.30 mm × 0.35 mm was picked up and used for the X-ray data collection. X-ray diffraction measurements were performed at 295 K on a Rigaku AFC7R diffractometer using a graphite-monochromated Cu Kα radiation (λ = 1.541 78 Å) and a rotating anode generator. Cell constants were obtained by least-squares refinement using the setting angles of 25 carefully centered reflections in the range of 45° < 2θ < 50°. Crystal data are as follows: space group $P2_12_12_1$, a = 20.432(1) Å, b = 23.575(1) Å, c = 6.628(5) Å, V = 3192.7(5) Å^3, Z = 4, D_{cal} = 1.272 g/cm^3. The 3491 reflections were collected (2θ × 140.2°) ω/2θ mode with ω scan width is (1.73 + 0.30tan θ)° and ω scan speed is 16.0°/min. The linear absorption coefficient, μ, for Cu Kα radiation is 7.37 cm^{-1}. The data were corrected for Lorentz and polarization effects. The structure was solved by direct methods[66] and expanded using Fourier techniques. The non-hydrogen atoms were refined anisotropically. Hydrogen atoms in the OH group were refined isotropically, while the rest were included in fixed positions. The final cycle of full-matrix least-squares refinement was based on 3461 observed reflections [I > 0.00σ(I)] and 447 variable parameters. Final R and weighted R values were 0.087 and 0.139, respectively. The maximum and minimum peaks on the final difference Fourier map corresponded to 0.40 and −0.26 e/Å^3, respectively. All calculations were performed using the teXsan[67] crystallographic software package of Molecular Structure Corporation. Atom coordinates, thermal parameters, bond lengths, and angles are available as Supporting Information.

Rat ET_A Receptors Binding Assay. The rat aorta smooth muscular cells were cultured on 48 well culture plates. After 3−5 days, the cluster medium was aspirated, and the cells were washed twice with ice-cold HEPES-buffered Hank's solution (20 mM, pH 7.4). The cells in each well were incubated with 12.5 pM [^{125}I]ET-1 in HEPES-buffered Hank's solution (0.3 mL) containing PMSF (0.1 mM), protinin (10 μg/mL), leupeptin (10 μg/mL), pepstatin A (10 μg/mL), bacitracin (250 μg/mL), and soybean trypsin inhibitor (10 μg/mL) in the absence or presence of a test compound at varying concentrations. Equilibrium binding studies were performed at 37 °C for 60 min. The incubation was terminated by rapid removal of the incubation medium and addition of ice-cold HEPES-buffered Hank's solution (0.25 mL). The free ligand was removed by washing the intact attached cells two times with ice-cold HEPES-buffered Hank's solution. The cells were dissolved in 0.1 M NaOH and transferred to a test tube, and then the radioactivity was counted. The nonspecific binding was determined in the presence of 10^{-7} M ET-1 and was about 5−10% of the total binding.

Pig ET_B Receptors Binding Assay. COS cells translated with cDNA encoding porcine ET_B type receptor (90 μM, 10^{-3}−10^{-4} cells in Hank's solution containing 20 mM HEPES buffer and protease inhibitors) was incubated with [^{125}I]ET-3 (25 pM, 10 μL) and a test solution (1 μL) at various concentrations at 37 °C for 60 min. The incubation was terminated by filtering through a Whatman GF/C glass fiber filter (presoaked in 1% polyethylene imine), which was washed four times with Tris-HCl (2.5 mL, 50 mM, pH 7.4), and the radioactivity was counted. Specific binding was calculated by subtracting the nonspecific binding obtained in the presence of 0.1 μM ET-3.

Human ET_A Receptors Binding Assay. Membranes of CHO cells expressing human ET_A receptor were purchased from DuPont New Nuclear (Boston, MA) and used according to the manufacture's instructions. The binding studies were performed in a manner similar to that for pig ET_B, except that [^{125}I]ET-3 was replaced by [^{125}I]-ET1.

Human ET_B Receptors Binding Assay. Membranes of CHO cells expressing human ET_B receptor were purchased from DuPont New Nuclear and used according to the manufacturer's instructions. The binding studies were performed in a manner similar to that for pig ET_B.

Pharmacokinetic Studies in Rats. On the 2 days before the experiment, the right jugular vein was cannulated with polyethylene tubing for venous blood collection under light anesthesia with ethyl ether. Antagonist was dissolved in a mixture of 10% v/v *N*,*N*-dimethylacetamide, 50% v/v poly(ethylene glycol) 400, and 40% v/v saline. The solution was administrated intravenously to nonfasted rats at a dose of 5 mg/2 mL/kg. Venous blood was collected at certain intervals after dosing.

Antagonist suspended in 0.5% hydroxypropyl cellulose (HPC-SL) solution was administrated orally to nonfasted rats at a dose of 30 mg/2 mL/kg. Venous blood was collected at certain intervals after dosing.

The concentration of antagonist in plasma was analyzed by HPLC method. Briefly, 100 μL of plasma was mixed with 200 μL of acetonitrile, following by shaking and centrifuging. The supernatant was analyzed.

The maximum plasma concentration (C_{max}) was defined as the highest value actually recorded, and the time to reach C_{max} was measured accordingly. The area under the curve was calculated by the trapezoidal rule. Pharamcokinetic parameters were calculated using the nonlinear least-squares regression program, "MULTI".

Acknowledgment. The authors are grateful to Dr. T. Konoike and K. Oda, Manufacturing Technology R & D Laboratories, and T. Yorifuji, S. Shinomoto, Y. Ide, T. Oya, M. Nishiuchi, and H. Kinoshita, Discovery Research Laboratories. We also thank H. Nakai and T. Iwata, Discovery Research Laboratories, for carrying out the X-ray crystallographic analysis and the CD spectra analysis, respectively.

Supporting Information Available: Melting points, ^{1}H NMR spectra, and elemental analysis for the assayed compounds, X-ray crystallographic data for the (1*S*,2*R*)-(+)-norephedrine salt of (*R*)-**48**, and CD spectra of (*R*)-**48**, (*R*)-**82**, and (*S*)-**82**. This material is available free of charge via the Internet at http://pubs.acs.org.

References

(1) Yanagisawa, M.; Kurihara, H.; Kimura, S.; Tomobe, Y.; Kobayashi, M.; Mitsui, Y.; Yazaki, Y.; Goto, K.; Masaki, T. A Novel Potent Vasoconstrictor Peptide Produced by Vascular Endothelial Cells. *Nature* **1988**, *332*, 411−415.

(2) Inoue, A.; Yanagisawa, M.; Kimura, S.; Kasuya, Y.; Miyauchi, T.; Goto, K.; Masaki, T. The Human Endothelin Family: Three Structurally and Pharmacologically Distinct Isopeptides Predicted by Three Separate Genes. *Proc. Natl. Acad. Sci. U.S.A.* **1989**, *86*, 2863−2867.

(3) Opgenorth, T. J.; Wu-Wong, J. R.; Shiosaki, K. Endothelin-Converting Enzymes. *FASEB J.* **1992**, *6*, 2653−2659.

(4) Xu, D.; Emoto, N.; Giaid, A.; Slaughter, C.; Kaw, S.; deWit, D.; Yanagisawa, M. ECE-1: A Membrane-Bound Metalloprotease That Catalyzes the Proteolytic Activation of Big Endothelin-1. *Cell* **1994**, *78*, 473−485.

(5) Masaki, T.; Yanagisawa, M.; Goto, K. Physiology and Pharmacology of Endothelins. *Med. Res. Rev.* **1992**, *12*, 391−421.

(6) Eguchi, S.; Hirata, Y.; Imai, T.; Marumo, F. Endothelin Receptor Subtypes are Coupled to Adenylate Cyclase via Different Guanyl Nucleotide-Binding Proteins in Vasculature. *Endocrinology* **1993**, *132*, 524−529.

(7) Arai, H.; Hori, S.; Aramori, I.; Ohkubo, H.; Nakanishi, S. Cloning and Expression of a cDNA Encoding an Endothelin Receptor. *Nature* **1990**, *348*, 730−732.

(8) Sakurai, T.; Yanagisawa, M.; Takuwa, Y.; Miyazaki, H.; Kimura, S.; Goto, K.; Masaki, T. Cloning of a cDNA Encoding a Nonisopeptide-selective Subtype of the Endothelin Receptor. *Nature* **1990**, *348*, 732−735.

(9) Davenport, A. P.; O'Reilly, G.; Kuc, R. E. Endothelin ET_A and ET_B mRNA and Receptors Expressed by Smooth Muscle in the Human Vasculature: Majority of the ET_A Subtype. *Br. J. Pharmacol.* **1995**, *114*, 1110−1116.

(10) Karne, S.; Jayawickreme, C. K.; Lerner, M. R. Cloning and Characterization of an Endothelin-3 Specific Receptor (ET_C Receptor) from *Xenopus Laevis* Dermal Melanophores. *J. Biol. Chem.* **1993**, *268*, 19126−19133.

(11) Saito, Y.; Nakao, K.; Mukoyama, M.; Imura, H. Increased Plasma Endothelin Level in Patients with Essential Hypertension. *N. Engl. J. Med.* **1990**, *322*, 205.

(12) Shichiri, M.; Hirata, Y.; Ando, K.; Emori, T.; Ohta, K.; Kimoto, S.; Ogura, M.; Inoue, A.; Marumo, F. Plasma Endothelin levels in Hypertension and Chronic Renal Failure. *Hypertension* **1990**, *15*, 493−496.

(13) Ishikawa, S.; Miyauchi, T.; Sakai, S.; Ushinohama, H.; Sagawa, K.; Fusazaki, N.; Kado, H.; Sunagawa, H.; Honda, S.; Ueno, H. Elevated Levels of Plasma Endothelin-1 in Young Patients with Pulmonary Hypertension Caused by Congenital Heart Disease are Decreased After Successful Surgical Repair. *J. Thorac. Cardiovasc. Surg.* **1995**, *110*, 271−273.

(14) Giaid, A.; Yanagisawa, M.; Langleben, D.; Michel, R. P.; Levy, R.; Shennib, H.; Kimura, S.; Masaki, T.; Duguid, W. P.; Stewart, D. J. Expression of Endothelin-1 in the Lungs of Patients with Pulmonary Hypertension. *N. Engl. J. Med.* **1993**, *328*, 1732−1739.

(15) Miyauchi, T.; Yanagisawa, M.; Tomizawa, T.; Sugishita, Y.; Suzuki, N.; Fujino, M.; Ajisaka, R.; Goto, K.; Masaki, T. Increased Plasma Concentrations of Endothelin-1 and Big Endothelin-1 in Acute Myocardial Infarction. *Lancet* **1989**, *2*, 53−54.

(16) McMurray, J. J.; Ray, S. G.; Abdullah, I.; Dargie, H. J.; Morton, J. J. Plasma Endothelin in Chronic Heart Failure. *Circulation* **1992**, *85*, 1374−1379.

(17) Cavero, P. G.; Miller, W. L.; Heublein, D. M.; Margulies, K. B.; Burnett, J. C., Jr. Endothelin in Experimental Congestive Heart Failure in the Anaesthetized Dog. *Am. J. Physiol.* **1990**, *259*, F312−F317.

(18) Tomita, K.; Ujiie, K.; Nakanishi, T.; Tomura, S.; Matsuda, O.; Ando, K.; Shichiri, M.; Hirata, Y.; Marumo, F. Plasma Endothelin Levels in Patients with Acute Renal Failure. *N. Engl. J. Med.* **1989**, *321*, 1127.

(19) Shibouta, Y.; Suzuki, N.; Shino, A.; Matsumoto, H.; Terashita, Z. I.; Kondo, K.; Nishikawa, K. Pathophysiological Role of Endothelin in Acute Renal Failure. *Life Sci.* **1990**, *46*, 1611−1618.

(20) Lerman, A.; Edwards, B. S.; Hallett, J. W.; Heublein, D. M.; Sandberg, S. M.; Burnett, J. C., Jr. Circulating and Tissue Endothelin Immunoreactivity in Advanced Atherosclerosis. *N. Engl. J. Med.* **1991**, *325*, 997−1001.

(21) Ohno, A.; Naruse, M.; Kato, S.; Hosaka, M.; Naruse, K.; Demura, H.; Sugino, N. Endothelin-specific Antibodies Decrease Blood Pressure and Increase Glomerular Filtration Rate and Renal Plasma Flow in Spontaneously Hypertensive Rats. *J. Hypertens.* **1992**, *10*, 781−785.

(22) Douglas, S. A.; Gellai, M.; Ezekiel, M.; Feuerstein, G. Z.; Elliott, J. D.; Ohlstein, E. H. Antihypertensive Actions of the Novel Nonpeptide Endothelin Receptor Antagonist SB 209670. *Hypertension* **1995**, *25*, 818−822.

(23) Watanabe, T.; Awane, Y.; Ikeda, S.; Fujiwara, S.; Kubo, K.; Kikuchi, T.; Kusumoto, K.; Wakimasu, M.; Fujino, M. Pharmacology of Non-peptide ET_A and ET_B Receptor Antagonist, TAK-044 and the Inhibition of Myocardial Infarct Size in Rats. *Br. J. Pharmacol.* **1995**, *114*, 949−954.

(24) Wang, Q.-D.; Li, X.-S.; Lundberg, J. M.; Pernow, J. Protective Effects of Non-peptide Endothelin Receptor Antagonist Bosentan on Myocardial Ischemic and Reperfusion Injury in the Pig. *Cardiovasc. Res.* **1995**, *29*, 805−812.

(25) Douglas, S. A.; Louden, C.; Vickery-Clark, L. M.; Storer, B. L.; Hart, T.; Feuerstein, G. Z.; Elliott, J. D.; Ohlstein, E. H. A Role for Endogenous Endothelin-1 in Neointimal Formation after Rat Carotid Artery Balloon Angioplasty. Protective Effects of the Novel Nonpeptide Endothelin Receptor Antagonist SB 209670. *Circ. Res.* **1994**, *75*, 190−197.

(26) Sakai, S.; Miyauchi, T.; Kobayashi, M.; Yamaguchi, I.; Goto, K.; Sugishita, Y. Inhibition of Myocardial Endothelin Pathway Improves Long-Term Survival in Heart Failure. *Nature* **1996**, *384*, 353−355.

(27) Brooks, D. P.; dePalma, P. D.; Gellai, M.; Nambi, P.; Ohlstein, E. H.; Elliott, J. D.; Gleasson, J. G.; Ruffolo, R. R. Nonpeptide Endothelin Antagonists: III. Effect of SB 209670 and BQ123 on Acute Renal Failure in Anesthetized Dogs. *J. Pharmacol. Exp. Ther.* **1994**, *271*, 769−775.

(28) Roux, S. P.; Clozel, M.; Sprecher, U.; Gray, G.; Clozel, J. P. Ro 47-0203, a New Endothelin Receptor Antagonist Reverses Chronic Vasospasm in Experimental Subarachnoid Hemorrhage. *Circulation* **1993**, *88*, I-170.

(29) Clozel, M.; Breu, V.; Gray, G. A.; Kalina, B.; Löffler, B.-M.; Burri, K.; Cassal, J.-M.; Hirth, G.; Müller, M.; Neidhart, W. Pharmacological Characterization of Bosentan, a New Potent Orally Active, Nonpeptide Endothelin Receptor Antagonist. *J. Pharmacol. Exp. Ther.* **1994**, *270*, 228−235.

(30) Kiowski, W.; Stüsch, G.; Hunziker, P.; Müller, P.; Kim, J.; Oechslin, E.; Schmitt, R.; Jones, R.; Bertel, O. Evidence for Endothelin-1-mediated Vasoconstriction in Severe Chronic Heart Failure. *Lancet* **1995**, *346*, 732−736.

(31) Fukami, T.; Nagase, T.; Fujita, K.; Hayama, T.; Niiyama, K.; Mase, T.; Nakajima, S.; Fukuroda, T.; Saeki, T.; Nishikibe, M.; Ihara, M.; Yano, M.; Ishikawa, K. Structure−activity Relationships of Cyclic Pentapeptide Endothelin A Receptor Antagonists. *J. Med. Chem.* **1995**, *38*, 4309−4324.

(32) Ihara, M.; Noguchi, K.; Saeki, T.; Fukuroda, T.; Tsuchida, S.; Kimura, S.; Fukami, T.; Ishikawa, K.; Nishikibe, M.; Yano, M. Biological Profiles of Highly Potent Novel Endothelin Antagonists Selective for ET_A Receptor. *Life Sci.* **1992**, *50*, 247−255.

(33) Sogabe, K.; Nirei, H.; Shoubo, M.; Nomoto, A.; Ao, S.; Notsu, Y.; Ono, T. Pharmacological Profile of FR139317, a Novel, Potent Endothelin ET_A Receptor Antagonist. *J. Pharmacol. Exp. Ther.* **1993**, *264*, 1040−1046.

(34) Ishikawa, K.; Ihara, M.; Noguchi, K.; Mase, T.; Mino, N.; Saeki, T.; Fukuroda, T.; Fukami, T.; Ozaki, S.; Nagase, T.; Nishikibe, J.; Yano, M. Biochemical and Pharmacological Profile of a Potent and Selective Endothelin-B Receptor Antagonist, BQ-788. *Proc. Natl. Acad. Sci. U.S.A.* **1994**, *91*, 4892−4896.

(35) Tanaka, T.; Tsukuda, E.; Nozawa, M.; Nonaka, H.; Ohno, T.; Kasa, H.; Yamada, K.; Matsuda, Y. RES-701-1, a Novel, Potent, Endothelin Type B Receptor-selective Antagonist of Microbial Origin. *Mol. Pharmacol.* **1994**, *45*, 724−730.

(36) Urade, Y.; Fujitani, Y.; Oda, K.; Watakabe, T.; Umemura, I.; Takai, M.; Okada, T.; Sakata, K.; Karaki, H. An Endothelin B Receptor Selective Antagonist: IRL 1038, [(Cys11-Cys-15)]-endothelin-1 (11−21). *FEBS Lett.* **1992**, *311*, 12−16.

(37) Cody, W. L.; Doherty, A. M.; He, J. X.; DePue, P. L.; Rapundalo, S. T.; Hingorani, G. A.; Major, T. C.; Panek, R. L.; Haleen, S. J.; Dudley, D. T.; LaDouceur, D.; Reynolds, E. E.; Hill, K. E.; Flynn, M. A.; Reynolds, E. E. Design of a Functional Hexapeptide Antagonist of Endothelin. *J. Med. Chem.* **1992**, *35*, 3301−3303.

(38) Cody, W. L.; Doherty, A. M.; He, J. X.; DePue, P. L.; Waite, L. A.; Topliss, J. G.; Haleen, S. J.; LaDouceur, D.; Flynn, M. A.; Hill, K. E.; Reynolds, E. E. The Rational Design of a Highly Potent Combined ET_A and ET_B Receptor Antagonist (PD145065) and Related Analogues. *Med. Chem. Res.* **1993**, *3*, 154−162.

(39) Masuda, Y.; Sugo, T.; Kikuchi, T.; Kawata, A.; Satoh, M.; Fujisawa, Y.; Itoh, Y.; Wakimasu, M.; Ohtaki, T. Receptor Binding and Antagonist Properties of a Novel Endothelin Antagonist, TAK-044 {Cyclo[D-α-aspartyl-3[(4-phenylpiperazin-1-yl)carbonyl]-L-alanyl-L-α-aspartyl-D-2-(2-thienyl)glycyl-L-leucyl-D-tryptophyl]disodium salt}, in Human Endothelin A and Endothelin B Receptors. *J. Pharmacol. Exp. Ther.* **1996**, *279*, 675−685.

(40) Clozel, M.; Breu, V.; Burri, K.; Cassal, J.-M.; Fischli, W.; Gray, G. A.; Hirth, G.; Loeffler, B. M.; Mueller, M.; Neidhart, W.; Ramuz, H. Pathophysiological Role of Endothelin Revealed by the First Orally Active Endothelin Receptor Antagonist. *Nature* **1993**, *365*, 759−761.

(41) Stein, P. D.; Hunt, J. T.; Floyd, D. M.; Moreland, S.; Dickinson, K. E.; Mitchell, C.; Liu, E. C. C.-K.; Webb, M. L.; Murugesan, N.; Dickey, J.; McMullen, D.; Zhang, R.; Lee, V. G.; Serafino, R.; Delaney, C.; Schaeffer, T. R.; Kozlowski, M. The Discovery of Sulfonamide Endothelin Antagonists and the Development of the Orally Active ET_A Antagonist 5-(Dimethylamino)-*N*-(3,4-dimethyl-5-isoxazolyl)-1-naphthalenesulfonamide. *J. Med. Chem.* **1994**, *37*, 329−331.

(42) Webb, M. L.; Bird, J. E.; Liu, E. C. K.; Rose, P. M.; Serafino, R.; Stein, P. D.; Moreland, S. BMS-182874 is a Selective, Nonpeptide Endothelin ET_A Receptor Antagonist. *J. Pharmacol. Exp. Ther.* **1995**, *272*, 1124−1134.

(43) Elliott, J. D.; Lago, M. A.; Cousins, R. D.; Gao, A.; Leber, J. D.; Erhard, K. F.; Nambi, P.; Elshourbagy, N. A.; Kumar, C.; Lee, J. A.; Bean, J. W.; DeBrosse, C. W.; Eggleston, D. S.; Brooks, D. P.; Feuerstein, G.; Ruffolo, R. R.; Weinstock, J.; Gleason, J. G.; Peishoff, C. E.; Ohlstein, E. H. 1,3-Diarylindan-2-carboxylic Acids, Potent and Selective Non-peptide Endothelin Receptor Antagonists. *J. Med. Chem.* **1994**, *37*, 1553−1557.

(44) Ohlstein, E. H.; Nambi, P.; Douglas, S. A.; Edwards, R. M.; Gellai, M.; Lago, A.; Leber, J. D.; Cousins, R. D.; Frazee, J. S.; Peishoff, C. E.; Bean, J. W.; Eggleston, D. D.; Elshourbagy, N. A.; Kumar, C.; Lee, J. A.; Yue, T.-L.; Louden, C.; Brooks, D. P.; Weinstock, J.; Feuerstein, G.; Poste, G.; Ruffolo, R. R.; Gleason, J. G.; Elliott, J. D. SB 209670, a Rationally Designed Potent Nonpeptide Endothelin Receptor Antagonist. *Proc. Natl. Acad. Sci. U.S.A.* **1994**, *91*, 8052−8056.

(45) Doherty, A. M.; Patt, W. C.; Edmunds, J. J.; Berryman, K. A.; Reisdorph, B. R.; Plummer, M. S.; Shahripour, A.; Lee, C.; Cheng, X.-M.; Walker, D. M.; Haleen, S. J.; Keiser, J. A.; Flynn, M. A.; Welch, K. M.; Hallak, H.; Taylor, D. G.; Reynolds, E. E. Discovery of a Novel Series of Orally Active Non-Peptide Endothelin-A (ET_A) Receptor-selective Antagonists. *J. Med. Chem.* **1995**, *38*, 1259−1263.

(46) Patt, W. C.; Edmunds, J. J.; Repine, J. T.; Berryman, K. A.; Reisdorph, B. R.; Lee, C.; Plummer, M. S.; Shahripour, A.; Haleen, S. J.; Keiser, J. A.; Flynn, M. A.; Welch, K. M.; Reynolds, E. E.; Rubin, R.; Tobias, B.; Hallak, H.; Doherty, A. M. Structure−Activity Relationships in a Series of Orally Active γ-Hydroxyl Butenolide Endothelin Antagonists. *J. Med. Chem.* **1997**, *40*, 1063−1074.

(47) Winn, M.; von Geldern, T. W.; Opgenorth, T. J.; Jae, H.-S.; Tasker, A. S.; Boyd, S. A.; Kester, J. A.; Mantei, R. A.; Bal, R.; Sorensen, B. K.; Wu-Wong, J. R.; Chiou, W. J.; Dixon, D. B.; Novosad, E. I.; Hernandez, L.; Marsh, K. C. 2,4-Diarylpyrrolidine-3-carboxylic Acids-Potent ET_A Selective Endothelin Receptor Antagonists. 1. Discovery of A-127722. *J. Med. Chem.* **1996**, *39*, 1039−1048.

(48) Opgenorth, T. J.; Adler, A. L.; Calzadilla, S. V.; Chiou, W. J.; Dayton, B. D.; Dixon, D. B.; Gehrke, L. J.; Hernandez, L.; Magnuson, S. R.; Marsh, K. C.; Novosad, E. I.; von Geldern, T. W.; Wessale, J. L.; Winn, M.; Wu-wong, J. R. Pharmacological Characterization of A-127722: An Orally Active and Highly Potent ET_A-Selective Receptor Antagonist. *J. Pharmacol. Exp. Ther.* **1996**, *276*, 473−481.

(49) Walsh, T. F.; Fitch, K. J.; Chakravarty, P. K.; Williams, D. L., Jr.; Murphy, K. A.; Nolan, N. A.; O'Brien, J. A.; Lis, E. V., Jr.; Pettibone, D. J.; Kivlighn, S. D.; Gabel, R. A.; Zingaro, G. J.; Krause, S. M.; Siegl, P. K. S.; Clineschmidt, B. V.; Greenlee, W. J. The Discovery of L-749,329, a Highly Potent, Orally Active Antagonist of Endothelin Receptors. *Abstract of Papers*; 208th American Chemical Society National Meeting, Washington, DC, August 21−25, 1994; MEDI 145.

(50) Williams, D. L., Jr.; Murphy, K. L.; Nolan, N. A.; O'Brien, J. A.; Pettibone, D. J.; Kivlighn, S. D.; Krause, S. M.; Lis, E. V., Jr.; Zingaro, G. J.; Gabel, R. A.; Clayton, F. C.; Siegl, P. K. S.; Zhang, K.; Naue, J.; Vyas, K.; Walsh, T. F.; Fitch, K. J.; Chakraarty, P. K.; Greenlee, W. J.; Clineschmidt, B. V. Pharmacology of L-754,-142, a Highly Potent, Orally Active, Nonpeptidyl Endothelin Antagonist. *J. Pharmacol. Exp. Ther.* **1995**, *275*, 1518−1526.

(51) Jae, H. S.; Winn, M.; Dixon, D. B.; Marsh, K. C.; Nguyen, B.; Opgenorth, T. J.; von Geldern, T. W. Pyrrolidine-3-carboxylic Acids as Endothelin Antagonists. 2. Sulfonamide-Based ET_A/ET_B Mixed Antagonists. *J. Med. Chem.* **1997**, *40*, 3217−3227.

(52) Pierre, L. N.; Davenport, A. P. Endothelin Receptor Subtypes and Their Functional Relevance in Human Small Coronary Arteries. *Br. J. Pharmacol.* **1998**, *124*, 499−506.

(53) Ohnishi, M.; Wada, A.; Tsutamoto, T.; Fukai, D.; Kinoshita, M. Comparison of the Acute Effects of a Selective Endothelin ET_A and a Mixed ET_A/ET_B Receptor Antagonist in Heart Failure. *Cardiovasc. Res.* **1998**, *39*, 617−624.

(54) Bryan, D. L.; Elliot, J. D. [(Benzodioxolyl)methyl]propenoates and Their Uses as Endothelin Receptor Antagonists. WO 9402474, 1994; *Chem. Abstr.* **1994**, *120*, 270460.

(55) Keenan, R. M.; Weinstock, J.; Finkelstein, J. A.; Franz, R. G.; Gaitanopoulos, D. E.; Girard, G. R.; Hill, D. T.; Morgan, T. M.; Samanen, J. M.; Hempel, J.; Eggleston, D. S.; Aiyar, N.; Griffin, E.; Ohlstein, E. H.; Stack, E. J.; Weidley, E. F.; Edwards, R. Imidazole-5-acrylic Acids: Potent Nonpeptide Angiotensin II Receptor Antagonists Designed Using a Novel Peptide Pharmacophore Model. *J. Med. Chem.* **1992**, *35*, 3858−3872.

(56) Wexler, R. R.; Greenlee, W. J.; Irvin, J. D.; Goldberg, M. R.; Prendergast, K.; Smith, R. D.; Timmermans, P. B. M. W. M. Nonpeptide Angiotensin II Receptor Antagonists: The Next Generation in Antihypertensive Therapy. *J. Med. Chem.* **1996**, *39*, 625−656.

(57) Nohara, A.; Umetani, T.; Sanno, Y. Studies on Antianaphylactic Agents-I. A Facile Synthesis of 4-Oxo-4*H*-1-benzopyran-3-carboxaldehydes by Vilsmeier Reagents. *Tetrahedron* **1974**, *30*, 3553−3561.

(58) Eisai Co., Ltd. Chromene-3-carboxylic Acids. Jpn. Kokai Tokkyo Koho. JP 8181580, 1981; *Chem. Abstr.* **1981**, *95*, 187007.

(59) Litkei, G.; Patonay, T.; Szliágyi, L.; Dinya, Z. Hydroxymethylation of Flavanones. *Org. Prep. Proceed. Int.* **1991**, *23*, 741−747.

(60) El-Ahl, A. S.; Elmorsy, S. S.; Elbeheery, A. H.; Amer, F. A. A Novel Approach for the Synthesis of 5-Substituted Tetrazole Derivatives from Primary Amides in Mild One-step Method. *Tetrahedron Lett.* **1997**, *38*, 1257−1260.

(61) Ishizuka, N.; Matsumura, K.; Hayashi, K.; Sakai, K.; Yamamori, T. An Efficient Method for the Preparation of Enantiomerically Pure *N*-Acylsulfonamides Having an Asymmetric Center at the α-Position: Condensation of Acid Chlorides and Arylsulfonamides Under Solid−liquid Two-phase Conditions. *Synthesis* **2000**, 784−788 and references therein.

(62) Kikuchi, T.; Mori, Y.; Yokoi, T.; Nakazawa, S.; Kuroda, H.; Masada, Y.; Kitamura, K.; Kuriyama, K. Structure and Absolute Configuration of Sargatriol, a New Isoprenoid Chromenol from a Brown Alga, *Sargassu tortile* C. Agardh. *Chem. Pharm. Bull.* **1983**, *31*, 106−113.

(63) Sakurawi, K.; Yasuda, F.; Tozyo, T.; Nakamura, M.; Sato, T.; Kikuchi, J.; Terui, Y.; Ikenishi, Y.; Iwata, T.; Takahashi, K.; Konoike, T.; Mihara, S.; Fujimoto, M. Endothelin Receptor Triterpenoid, Myriceric Acid A, Isolated from *Myricsa cerifera*, and Structure Activity Relationships of Its Derivatives. *Chem. Pharm. Bull.* **1996**, *44*, 343−351.

(64) Davis, A. M.; Teague, S. J. Hydrogen Bonding, Hydrophobic Interactions, and Failure of the Rigid Receptor Hypothesis. *Angew. Chem., Int. Ed.* **1999**, *38*, 736−749.

(65) The pA_2 value of **(*R*)-48** for ET_A receptor-mediated constrictions in isolated rabbit femoral artery was 8.8. Orally administrated **(*R*)-48** caused dose-dependent inhibition of the pressure response to exogenous ET-1 in conscious normoretensive rats. In this case, the inhibitory effects at 0.3−10 mg/kg were 40−60% at 0.5 h, and its effects lasted for 4.5 h. Furthermore, oral administration of **(*R*)-48** at 10 mg/kg reduced systolic blood pressure appropriately 25 and 40 mm Hg after 6 and 10 h, respectively, in deoxycorticosterone acetate−salt hypertensive rats. Iwasaki, T.; Mihara, S.; Shimamura, T.; Kawakami, M.; Masui, M.; Hayasaki-Kajiwara, Y.; Naya, N.; Ninomiya, M.; Fujimoto, M.; Nakajima, M. Pharmacologic Characterization of S-1255, a Highly Potent and Orally Active Endothelin A Receptor Antagonist. *J. Cardiovasc. Pharmacol.* **2001**, *37*, 471−482.

(66) Altomare, A.; Burla, M. C.; Camalli, M.; Cascarano, M.; Giacovazzo, C.; Guagliardi, A.; Polidori, G. SIR92-a Program for Automatic Solution of Crystal Structures by Direct Methods. *J. Appl. Crystallogr.* **1994**, *27*, 435.

(67) teXsan, Crystal Structure Analysis Package (Molecular Structure Corporation, 1985 and 1992).

JM010382Z